1	
2	
3	
4	<b>Turbulence and Coral Reefs</b>
5	
6	
7	
8	
9	
10	Kristen A. Davis <sup>1*</sup> , Geno Pawlak <sup>2</sup> , and Stephen G. Monismith <sup>3</sup>
11	
12	<sup>1</sup> University of California, Irvine, Irvine, California, USA
13	<sup>2</sup> University of California, San Diego, La Jolla, California, USA
14	<sup>3</sup> Stanford University, Stanford, California, USA
15	
16	
17	
18	
19	A submission to Annual Reviews of Marine Science
20	
21	
22	
23	
24	
25	
26	
27	
28	
29	* corresponding author, Kristen A. Davis, davis@uci.edu
30	

# Abstract (150 words) The interaction of coral reefs, both chemically and physically, with the surrounding seawater is governed, at the smallest scales, by turbulence. Here we review recent progress in understanding turbulence in the unique setting of coral reefs - how it influences flow and the exchange of mass and momentum both above and within the complex geometry of coral reef canopies. Flow above reefs diverges from canonical rough boundary layers due to their large and highly heterogeneous roughness and the influence of surface waves. Within coral canopies, turbulence is dominated by large coherent structures which transport momentum both into and away from the canopy but

is also generated at smaller scales as flow is forced to move around branches or blades creating

wakes. Future work should carefully consider the influence of spatial variations on the fluxes of

momentum and scalars in interpreting observations in reef environments and in applying these to

numerical models.

50 H

Key Words (6): turbulence, coral reefs, rough boundary layers, mass transfer, canopy flow,

51 waves

### 52 1.0 Introduction 53 Coral reefs are among the most diverse ecosystems on the planet (Veron 1995). They play an 54 important role protecting coastlines from the damaging effects of waves, provide nurseries for 55 many ocean fish species, and represent a vital source of food for developing nations (Ferrario et 56 al. 2014; Burke et al. 2011). Additionally, reefs are biogeochemical "reactors", where the high 57 metabolism of the benthic community transforms and recycles carbon, nitrogen, and other 58 nutrients for marine food chains (D'elia & Wiebe 1990). The interaction of coral reefs, both 59 chemically and physically, with the surrounding seawater is governed by flow - at the large 60 scales by tides, mesoscale currents, and waves and at the smallest scales by turbulence. 61 62 Oceanic forcing shapes regional circulation patterns and the horizontal transport of water masses 63 with different properties to the reef, governing the environmental conditions and the dispersal of 64 reef larvae and, thus, the biogeographical distribution of reef organisms (reviewed in Lowe & 65 Falter 2015). However, turbulent mixing governs the vertical "coupling" between the bed and 66 the overlying water - determining the vertical transport of heat, food, pollutants, pathogens, 67 larvae, or nutrients to or from the benthic reef community (Thomas & Atkinson 1997; Falter et 68 al. 2004, 2007; Monismith et al. 2010; Sebens et al. 1998, 2003, Reidenbach et al., 2009). A 69 review of reef-scale hydrodynamics and boundary layer flows over reefs can be found in 70 Monismith (2007). Here, however, we focus on the smallest scales of water motion on coral 71 reefs - turbulence. 72 73 This review is motivated, in part, by a defining physical characteristic of coral reefs that makes 74 them a good place to study turbulence - their extreme hydrodynamic roughness. While natural 75 surfaces under the erosive influence of breaking waves and strong currents would tend to be 76 worn smooth, scleractinian (hard) corals actively grow complex structures (i.e. "roughness 77 elements" to fluid dynamicists!) that induce mixing and enhance turbulent fluxes near the bed 78 (e.g. van Woesik et al 2012). The geometric complexity of corals can be seen at the scale of 79 individual coral colonies with their various morphologies (e.g. branching, foliated, massive, and 80 encrusting forms), to the scale of reef platforms where steeply sloping forereefs cut with spur-

and-groove formations differ greatly from the wide, shallow reef flats, and bommie-filled

lagoons in (Figure 1). Spatially-variable reef structure creates correspondingly complex

81

83 hydrodynamic regimes that are shaped, in part, by the relative height of the coral reef canopy,  $h_c$ , 84 relative to the depth of the water column, h, and the relative strength of wave-driven flows,  $U_w$ , 85 to mean, unidirectional currents,  $U_c$  (Figure 2). 86 87 Structural complexity creates manifold microhabitats and is thought to be a key feature 88 influencing ecological processes on reefs - affecting the availability of food and the abundance of 89 fish, enhancing herbivory by reef fishes to reduce algae cover, and providing shelter from 90 predators (Holbrook et al. 2002; Gratwicke & Speight, 2005; Harborne et al. 2012; Graham & 91 Nash 2013). The interdisciplinary nature of science on coral reefs has led to various methods for 92 defining and quantifying the structural complexity of the benthic community. One of the most 93 common methods of quantifying bottom roughness in marine ecological studies is the "chain-94 and-tape" estimate of rugosity, which is the ratio of the contour length along the substrate surface 95 to the corresponding projected horizontal length (Risk 1972). Recent efforts to quantify the 96 complex, multiscale benthic topography of coral reefs have found success in fractal theory 97 (Zawada & Brock, 2009; Duvall et al. 2019). Hydrodynamic studies quantify roughness as 98 standard deviation (Lowe et al. 2005a), root-mean-square slope (Rogers et al. 2018), or 99 'roughness density', the total frontal area of canopy elements per horizontal area (Schlichting 100 1937, Dvorak 1969, Wooding 1973, Jimenez 2004). But, most often, physical oceanographers 101 are interested in how the 'roughness elements' of the benthic reef community impose large 102 bottom stresses on the flow, characterizing this effect through drag coefficients  $(C_D)$ , 103 hydrodynamic roughness ( $z_0$ ), and friction factors ( $f_w$ ,  $f_e$ ) (Lowe et al. 2005a; Monismith 2007). 104 For example, estimates of drag coefficients over coral reef communities commonly find values 105 one to two orders of magnitude higher than that for sandy or muddy coastal beds (Heathershaw 106 & Simpson 1978; Lugo-Fernandez et al. 1998; Lentz et al. 2017). 107 108 This review focuses on recent progress in understanding turbulence in the unique setting of coral 109 reefs. We develop a mathematical framework for our discussion in Section 2. We draw insights 110 from relevant engineering literature on flow over rough surfaces and studies of atmospheric flow 111 over vegetation and urban canopies in Section 3. The shallow setting of many reef environments 112 requires consideration of the influence of the free-surface and waves on turbulent flows (Section 113 4). For reefs exposed to internal waves, stratified turbulent boundary layer dynamics become

relevant (Section 5). We consider turbulent flow within coral canopies (Section 6) as it is important for mass transport (Section 7), predation of corals by fish, particle capture by corals, and larval settlement.

# 2.0 The analysis framework

Here we present the equations governing flow in and above coral canopies and define some useful terms and notations that will be used throughout the paper. We adopt right-handed Cartesian coordinates where x = [x,y,z] represents the three-dimensional spatial coordinate axes and u = [u,v,w] is the corresponding velocity vector. For the simplest case of unidirectional flow, turbulent quantities can be represented using a Reynolds decomposition of the velocity vector and other scalar quantities, shown here for the u-component of velocity, as:

$$u = \overline{u} + u' \tag{1}$$

where the overbar represents a time-average and the prime denotes a fluctuating, or turbulent, quantity. Using this notation within the equation for conservation of momentum and taking the time-average results in the Reynolds-averaged Navier Stokes equation, here presented in two dimensions - x, streamwise horizontal and parallel to the bed, and z, normal to the bed (z = 0 at the bed):

$$\frac{D\overline{u}}{Dt} = -\frac{1}{\rho} \frac{\partial \overline{p}}{\partial x} + \frac{1}{\rho} \frac{\partial \tau_{xz}}{\partial z}$$
(2)

where t is time, p is pressure,  $\rho$  is the fluid density, and  $\tau_{xz}$  is defined here as a sum of the Reynolds stress and the viscous stress:

$$\tau_{xz} = -\rho \overline{u'w'} + \mu \frac{\partial \overline{u}}{\partial z} \tag{3}$$

where  $\mu$  is fluid viscosity. Equation 2 is relevant for unidirectional flow above canopies, but surface gravity waves are a common feature of coral reef habitats. Oscillatory wave-driven flow can significantly enhance turbulence in a region near the bed called the wave boundary layer (Grant & Madsen 1986; Trowbridge & Lentz 2018). Turbulent motions in the presence of waves

complicate the usual Reynolds decomposition for velocity, with the introduction of wavecorrelated motions:

$$u = \overline{u} + \tilde{u} + u' \tag{4}$$

where the second term,  $\tilde{u}$ , added relative to Equation 1, represents motions that are coherent with the wave phase.

The time-averaged vertical stress in the presence of waves includes an extra stress (relative to Equation 4) that is due to the temporal correlation of oscillatory velocities:

$$\tau_{xz} = -\rho \overline{u'w'} - \rho \overline{\tilde{u}\tilde{w}} + \mu \frac{\partial \overline{u}}{\partial z}. \tag{5}$$

For high Reynolds numbers, typical for reef environments, the last term in Equations 4 and 5 is generally negligible. Other stress terms ( $\tau_{xx}$ ,  $\tau_{yy}$ ,  $\tau_{xy}$ ), not written out here, will also be relevant in regions of flow with significant variability in the horizontal or in the presence of waves and include terms important to the wave radiation stress (Longuet-Higgins & Stewart 1964).

Within the canopy, the effect of the roughness elements is felt more directly, as flow must move around coral branches, heads, blades of macroalgae, and other canopy elements, creating a highly variable spatial flow structure that is challenging to characterize - even for the simplest geometric approximations of canopy elements (Lowe et al., 2005b). To represent the effect of this complex instantaneous flow field on the mean velocities within the canopy, it is common to employ a double-averaging method with the Reynolds-averaged Navier Stokes equations - both in time, as is commonly done, and in space over a horizontal plane to remove element-scale spatial heterogeneity (Raupach & Shaw 1982). Using this idea, time-averaged quantities are further broken down as,

$$\overline{u} = \langle \overline{u} \rangle + u'' \tag{6}$$

where brackets denote a spatial average over a horizontal plane (excluding the solid parts of the canopy elements), and double-primes denote deviations from the spatial mean. The double-averaged, 2D momentum equation for unidirectional flow within a canopy becomes,

$$\frac{D\langle \overline{u} \rangle}{Dt} = -\frac{1}{\rho} \frac{\partial \langle \overline{p} \rangle}{\partial x} + \frac{1}{\rho} \frac{\partial \langle \tau_{xz} \rangle}{\partial z} - F_x \tag{7}$$

where,

$$\langle \tau_{xz} \rangle = -\rho \left\langle \overline{u'w'} \right\rangle - \rho \left\langle \overline{u}'' \overline{w}'' \right\rangle + \mu \frac{\partial \left\langle \overline{u} \right\rangle}{\partial z} \tag{8}$$

is the spatially-averaged total stress, in which an extra term,  $\langle \overline{u}''\overline{w}'' \rangle$ , called the "dispersive stress" appears, that accounts for the spatial correlations in the time-averaged velocity field. The last term in Equation 7,  $F_x$ , represents the spatially-averaged drag force exerted by the canopy elements onto the surrounding flow.

# 3.0 Turbulence and mixing over rough terrain

Turbulence in coral reef environments arises through a variety of mechanisms including breaking surface waves, breaking internal waves, boundary layers over coral elements and free shear layers from separated flows around those elements. The latter two mechanisms are distinctive to coral reefs relative to other environmental settings due to the extreme, complex nature of coral surfaces. Flows over terrestrial vegetated canopies (i.e. Belcher et al. 2012) are most similar, though the ubiquity of oscillatory motion due to surface waves sets coral reefs further apart.

The key quantity that characterizes the turbulence and overall structure for unstratified flow interaction with a boundary is the net rate of loss of fluid momentum or equivalently, the drag force that the boundary exerts on the fluid. This is generally given in terms of force per unit area as a total stress,  $\tau_b$ , which is manifested at the boundary via viscous shear stress and pressure drag on roughness elements. For rough boundaries at high Reynolds numbers, the latter is dominant (Jimenez 2004). The total stress is also given in terms of a friction velocity  $u_* = \sqrt{\tau_b/\rho}$  where  $\rho$  is water density. The drag (D) on the flow (per unit area,  $A_T$ ) is given, using a quadratic drag law as:

$$\tau_b = \frac{D}{A_T} = \rho C_D U^2 \tag{9}$$

where U is a suitably defined reference velocity often chosen based on a reference height or using a depth average. This choice, of course, can result in differing values for the drag coefficient,  $C_D$ , and potentially complicates comparison between reported measurements (Rosman & Hench 2011).

Starting with canonical considerations of unstratified steady and oscillatory flow interaction with a rough boundary (c.f. Grant & Madsen 1986, Trowbridge & Lentz 2018), we can identify a suite of relevant dimensionless parameters that will describe the interaction of flow with reef roughness and subsequent turbulent flow characteristics:

$$u_* = u_* \left( U_c / U_w, \phi_{wc}, k / h, k / A, P \right) \tag{10}$$

The first parameter represents the relative magnitude of steady  $(U_c)$  to oscillatory  $(U_w)$  velocities. The second parameter,  $\phi_{wc}$ , is the relative angle between waves and steady flow. The third and fourth parameters relate a characteristic physical roughness length scale, k, to the total water depth, k, and to the wave orbital amplitude, k0 amplitude, k1 and to the wave orbital amplitude, k2 amplitude, k3 and the influence of the reef surface geometry on the flow. Reef surfaces are inherently multiscaled, so that the choice for the characteristic scale, k3, and its connection to the hydrodynamics is not immediately clear. The last parameter k2 then represents some measure (or set of measures) that captures the effects of the complex distribution of roughness scales on the flow. As discussed further below, these measures can include spectral distributions, solidity, and roughness density among others.

Because relevant velocity and roughness scales are large, reefs are assumed to be *fully rough* so the Reynolds number is not typically considered as a parameter. Near coral surfaces, at the scale of individual coral communities and within canopies, viscous effects will likely play important roles.

# 3.1 Canonical rough boundary layer

In the classic paradigm for flow over a homogeneously rough boundary, at some distance above the bed, the flow depends only on  $u^*$ , some characteristic length scale for the roughness,  $z_0$ , and distance from the boundary, z. Dimensional considerations then require that the time-averaged velocity U(z) follow a logarithmic profile:

$$\frac{U(z)}{u_*} = \frac{1}{\kappa} \ln \frac{z}{z_0} \tag{11}$$

(Pope 2000) where  $\kappa \sim 0.4$  is the von Kármán constant (Long et al. 1993, Bailey et al. 2014). Equation 11, an expression of the so-called *law of the wall*, applies where the distance from the wall is much greater than the roughness scale,  $z \gg z_0$  and much smaller than the overall boundary layer thickness,  $\delta$ . The length scale  $z_0$  in the log profile, is more accurately the *hydrodynamic roughness*, and represents the height at which the average velocity would vanish if extrapolated downward. This quantity is typically determined from empirical fits of Equation 11 to measured velocity profiles. In actuality, the velocity near  $z\sim z_0$  is modified by details of the roughness and, especially for coral reefs, by the turbulent wave boundary layer. The relation between the hydrodynamic roughness length and a representative physical roughness scale k introduced in Equation 10 is not explicit, however. A relation for sand grain roughness, obtained by Nikuradse (1933), is commonly used for homogenous roughness:  $z_0 = k_s/30$ , where  $k_s$  is a characteristic sand grain size. For more complex roughness characterized by multiple length scales, the transfer function is not so clear, as will be discussed further below.

Large and highly variable roughness for coral reef surfaces complicates the definition of the vertical coordinate in Equation 11. An arbitrarily defined vertical coordinate z' can be related to the coordinate z in Equation 11 introducing the *hydrodynamic origin* or *displacement height*,  $z_{ref} = z-z'$  (Raupach et al. 1991). Jackson (1981) showed that this location corresponds to the height at which the hydrodynamic drag force is applied to the surface. For widely spaced, regular transverse square bars, Leonardi et al. (2003) showed that this was at roughly half of the element height.

The parameters in Equation 11 are defined differently across various fields of application, for example, in engineering literature, the velocity offset associated with  $z_0$  is commonly given as a 'roughness function'  $\Delta U^+$ , and Equation 11 is expressed as

$$U^{+} = \frac{1}{\kappa} \ln z^{+} - \Delta U^{+} \tag{12}$$

Here + refers to nondimensional values scaled using a viscous length  $v/u_*$  so that  $U^+ =$ 

 $U(z)/u_*$  and  $z^+ = zu_*/v$ . The roughness function then is related to the reduction in the velocity

profile for the rough boundary case relative to that for a smooth wall (Jimenez 2004).

outer layer. The velocity profile across the layer is then represented by:

263

Equations 11 and 12 apply within a limited region near the boundary where the overall boundary layer thickness is not yet relevant. For open channel flows where the boundary layer is 'fully-developed' so that the boundary effects extend throughout the water column, Equations 11 and 12 can accurately describe velocity profiles for z < 0.2h (Nezu & Nakagawa 1993). Outside of this region, the deviation of the mean velocity from the log profile can be accounted for by addition of a *wake function* or *velocity defect law* (Coles 1956) that adjusts for dynamics in the

271

270

$$\frac{U(z)}{u_*} = \frac{1}{\kappa} \left( \ln \frac{z}{z_0} + 2\Pi \sin^2 \left( \frac{\pi}{2} \frac{z}{\delta} \right) \right). \tag{13}$$

273274

275

276

277

278

Here,  $\Pi$  is a flow dependent wake strength parameter. For fully developed flow,  $\delta = h$  in Equation 13, and  $\Pi \simeq 0.2$  (Nezu & Nakagawa, 1993). The presence of a free surface can affect turbulent flow differently, suppressing vertical turbulent motions and modifying the velocity profile relative to that near the centerline in a closed channel or at the upper edge of a developing boundary layer (see Talke et al. 2013). Guo & Julien (2007) developed a modified wake function that accounts for a near-surface reduction in velocity for open-channel flow.

279280

If we consider  $C_D$  from Equation 9 defined using the depth averaged velocity and assume fully developed flow and  $k \ll h$  so that Equation 13 applies over the full depth, then the drag coefficient can be related to the hydrodynamic roughness as:

 $C_D \approx \kappa^2 \left[ \ln \left( \frac{h}{z_0} \right) + (\Pi - 1) \right]^{-2}$ 284 (14)285 where the drag coefficient then varies as function of depth, for a given roughness (Lentz et al. 286 2017). 287 288 Details and consequences associated with the logarithmic profile have been discussed 289 extensively elsewhere (Grant & Madsen 1986; Jimenez 2004; Trowbridge & Lentz 2018). The 290 validity of Equations 11-13 has been verified in multiple settings (Lueck & Lu 1997; Sanford & 291 Lien 1999), although values of the shear stress derived from the law of the wall and 292 measurements of the shear stress made using other means, e.g. from the variance method (Stacey 293 et al. 1999), sometimes do not agree. Nonetheless, the law of the wall has several useful features: 294 (1) As evident in Equation 14 and shown by Lentz et al. (2017), the dependence of drag 295 coefficients for depth-averaged flows on  $h/z_0$  can be obtained where roughness scales are 296 assumed to be much smaller than the overall depth (similar behavior was observed by McDonald 297 et al. (2006) for cases where the coral canopy was a sizable fraction of the total depth). 298 (2) As will be discussed below, the assumed eddy diffusivity variation with height appropriate to 299 law of the wall can be used with measurements of bulk concentration gradients of scalars, like 300 total alkalinity or temperature for example, to infer fluxes. 301 302 In the context of coral reefs, several factors put the validity of Equations 11-13 into question, 303 however, including large and highly heterogeneous roughness and the influence of surface 304 waves. 305 306 3.2 Turbulence over highly irregular roughness 307 The parameter P in the functional relation in Equation 10 represents some quantitative measure 308 (or set of measures) of irregular reef roughness that captures the connection between the complex 309 multiscaled surface and the hydrodynamic roughness  $z_0$  in Equation 11. A number of measures 310 have been proposed in engineering studies of rough boundaries including root-mean-square (rms) height, spectral moments, roughness slope, among others (see Schultz & Flack 2009 and 311

references therein). As summarized by Schultz & Flack (2009), "Even with modest success of

these correlations for a specific roughness type, it can be concluded that, at present, there is no

312

sufficiently satisfactory scaling for a generic, three-dimensional roughness". The situation is more acute when considering complex roughness associated with coral reef canopies.

We can nonetheless obtain some guidance on how to approach roughness parameterization from considering regular roughness arrays. Considering a single, bluff body of height k and transverse width s on a flat bottom within a steady mean flow U, the total pressure drag should be well-described using a drag coefficient of order 1 and using the frontal area k\*s. If we consider a regular array of these elements, sparsely spaced at intervals of w and b in the longitudinal and lateral directions, respectively, then the total drag per unit area is

$$\frac{D}{A_T} \sim \rho U^2 \frac{ks}{bw} \sim \rho U^2 \lambda \tag{15}$$

Roughness slope has been used successfully to describe drag for reef surfaces. Rogers et al. (2018) used a numerical model to examine flow over a reef surface obtained from high resolution topographic measurements from a shallow reef flat in American Samoa with relatively sparse coral coverage. Model drag estimates agreed well with observed values and were well predicted using Equation 14 with  $z_0$  based on rms roughness and an average roughness slope.

For the regular roughness case, as element spacing is reduced, flow sheltering begins to play a role, reducing the relative flow velocity and complicating the relationship with  $\lambda$ . When spacing is reduced so that k-w, the full element height k is no longer relevant for drag. This is the  $\delta$ -type roughness regime identified by Perry et al. (1969). Leonardi et al. 2003 showed that for w<5k the hydrodynamic origin approaches ~0.1w below the top of the roughness elements. This can be

interpreted as a critical cavity aspect ratio  $w/k\sim5$  below which the outer flow no longer responds to the lower part of the cavity geometry. For  $\delta$ -type roughness then, the full roughness density is no longer relevant in Equation 15 and the roughness element spacing w must play a role in setting the hydrodynamic roughness.

Rajagopalan (2010) applied the critical cavity aspect ratio paradigm to 2D irregular roughness to determine the hydrodynamic origin  $\zeta_0$  relative to the top of the roughness, based on an effective cavity aspect ratio for the irregular bed. For the 2D case, the hydrodynamic roughness was given by  $z_0 \sim \zeta_0 \left(1 - \lambda_{\zeta_0}\right)$  where  $\lambda_{\zeta_0}$  is a modified roughness density measured down to  $\zeta_0$ . This idea is consistent with an alternate empirical roughness density  $\lambda_s$  that adjusts for the 'windward wetted surface area' (Sigal & Danberg 1990, van Rij et al. 2002). Numerous relationships between  $z_0$  and  $\lambda$  and  $\lambda_s$  have been determined empirically for a range of 2D and 3D bed geometries, as reviewed by Flack & Schultz (2010).

Roughness measurements show that coral reefs are commonly multiscaled (Zawada & Brock 2009; Duvall et al. 2019) with roughness distributions that can be described by a red spectral distribution (Nunes & Pawlak 2008; Jaramillo & Pawlak 2011; Amador et al. submitted A) over a range of scales spanning O(10 cm) to O(10 m). In order to resolve the relevant spectral range, Reidenbach et al. (2006) covered a section of reef with plastic sheeting effectively eliminating fine scale roughness and found that drag and turbulence was unchanged. The Eilat forereef they considered (**Figure 2b**) could be described as a sparse canopy with a set of isolated obstacles with k/h >> 1 so results may not be broadly applicable to more dense canopies, but their observations suggest that the larger roughness scales are dominant in the mean flow drag response.

At the lower end of the spectrum, the transition between the scales that contribute to roughness and those that can be considered bathymetry is not obvious for reef topography. Conceptually, we might consider scales that lead to flow separation as contributing to roughness, with longer length scales driving a potential flow response. Schultz & Flack (2009) noted that roughness with an average slope less than 0.35 did not map onto the hydrodynamic roughness, denoting lower slopes as 'wavy' surfaces. Spatial drag measurements by Amador et al. (submitted A)

over a sparsely covered forereef were best correlated with spectral roughness rms for wavelengths greater than 20 m (for depths of 5-30 m) suggesting that the larger roughness scales were most relevant in determining drag, consistent with Reidenbach et al. (2006). The apparent discrepancy between these results and Schultz & Flack's (2009) critical slope may be associated with the fact that, for coral reefs, longer wavelengths are more likely coincident with sharp changes, as for spur and groove topography (Storlazzi et al. 2003), that are manifested in broad spectral distributions.

Where  $k \ll h$ , we can explore whether the overlying flow can be at least in local equilibrium with the local bed roughness. Studies of rough wall turbulence have shown that the boundary layer thickness must satisfy  $\delta/k_s \gg 40$ , where  $k_s$  is the equivalent sand grain roughness, for the turbulence similarity assumptions that underlie Equation 11 to be valid (Jimenez 2004, Flack et al. 2005). Where this condition is not met, turbulence may be more characteristic of that for flow over obstacles. Nevertheless, velocity profiles have been shown to be well-described by logarithmic structure in many high roughness coral reef environments and yield bed stresses that agree with other methods (Reidenbach et al 2006; Lentz et al. 2017; Arzeno et al. 2018, Amador et al. submitted A). Spatially averaged drag estimates by Amador et al. (submitted A) yielded values that compared reasonably well with log fit and Reynolds stress estimates at one of two fixed sites. At a second site, where advection was notable, the comparison was poorer. At both sites, however, Reynolds stress profiles showed relatively weak connection with local shear, indicating nonequilibrium conditions (Amador et al. submitted B).

The high spatial heterogeneity that characterizes coral reef environments poses a challenge for interpreting field observations traditionally obtained from a single location. It also represents a practical problem for numerical modeling where model grid cells require averaging over variable roughness. These issues are similar to those associated with atmospheric flow over variable topography and associated studies can provide some guidance in understanding turbulence in coral reefs. Meteorologists use the blending height  $\delta_b$  as a measure of the vertical extent at which effects of surface heterogeneities are no longer discernible (Mahrt, 2000). Mason (1988) described the blending height as the level at which a change in bed stress is balanced by a corresponding perturbation in advection which gives  $\delta_b = C_b L_c \left(u_*/U_{\delta_b}\right)^2$  where  $L_c$  is a

406 characteristic horizontal scale for heterogeneity,  $U_{\delta_h}$  is the velocity at the blending height and  $C_b$ 407 is a constant of order 1. Alternately, the blending height has also been defined using a diffusive length argument (Claussen 1990) as  $\delta_b = C_b L_c (u_*/U_{\delta_b})$ . The blending height can be 408 interpreted as the height above a homogenous patch of roughness to which the flow can be 409 410 considered in local equilibrium. For coral reef flows with depth h, and typical steady flow drag coefficients  $C_D \sim 10^{-2}$  (Lentz et al. 2017), these relations suggest that heterogeneity at scales less 411 than  $L_c = 10-100 h$  will lead to turbulence that is not in equilibrium with the local roughness. 412 413 Given the roughness regimes that are represented in **Figure 2**, we can anticipate that spatial 414 variability will play an important role in turbulence for many reef environments. In these cases, 415 local advective contributions to momentum balances and to turbulent fluxes will be important. 416 417 Spatial variability brings about additional complications in parameterizing turbulent stresses over 418 reef scales due to the role of persistent spatial flow structure. As shown by Mahrt (1987) for 419 numerical modeling of atmospheric flow, this spatial structure contributes to subgrid fluxes that 420 appear via the dispersive stress in Equation 8. For coral reefs, specific mechanisms for spatially 421 variable, persistent flow can include local advection and acceleration around individual 422 roughness elements and reef topography (Hench & Rosman 2013; Rogers et al. 2015), waveinduced residuals (Pawlak & MacCready 2002) and thermally driven flows (Monismith et al. 423 424 2006, Molina et al. 2014). 425 426 Taylor (1987) noted a similar issue in averaging of variable roughness noting that the spatiallyaveraged hydrodynamic roughness length is given by  $\ln z_{0_a} = \left[u_* \ln z_0\right]/\left[u_*\right]$  . Using a 427 Taylor series expansion, this can be approximated as  $\ln z_{0a} \approx [\ln z_0]$  which avoids averaging 428 429 over the shear stress velocity. These relations highlight the complications that must be 430 considered in interpreting local observations and in applying these to numerical models. 431 432 Extrapolating the approaches from atmospheric boundary layers neglects effects due to surface 433 waves that are intrinsic for many reef environments. Wave effects on current boundary layer 434 structure in heterogeneous roughness have not previously been considered in detail.

### 4.0 Surface waves and the wave boundary layer

Surface waves drive oscillatory motions that can often be larger than steady flows in many reef environments (Monismith 2007). The effects of irrotational surface wave motion on turbulence generated by steady flow over the rough seabed is commonly neglected although Teixeira & Belcher (2002) have shown that wave induced strain and Stokes drift shear can result in time variable modulation of Reynolds stresses and anisotropy. Near the bed, the periodic motions directly drive turbulence and indirectly modify the mean flow.

The vertical extent of the bottom boundary layer associated with wave driven motions is limited by the wave period so that vertical gradients in velocity along with corresponding stresses and turbulent intensities are much higher than for comparable steady flows (Grant & Madsen 1979). For sediment seabeds, wave boundary layer thicknesses are on the order of centimeters (Grant & Madsen 1986, Trowbridge & Lentz 2018). For rough beds, however, the turbulent wave boundary layer extent is determined by the height of the roughness elements, which for coral reefs can range from centimeters to meters (c.f. **Figure 2**).

Similarly to the thicker steady flow boundary layer, turbulence within the wave-driven boundary layer can be related to the time variable shear stress velocity. The magnitude of the corresponding time varying stress is typically parameterized using a wave friction factor,  $f_w$ , as:

$$\tau_{w_m} = \frac{1}{2} \rho f_w U_w^2 \tag{16}$$

(Jonsson 1966). Extensive work has been carried out towards developing parameterizations for  $f_w$  over homogeneously rough beds with  $k/A \ll 1$ , primarily in the context of coastal engineering and sediment transport applications. The majority of these studies build on the original formulation by Jonsson (1966), later modified by Swart (1974) and examined experimentally by Kamphuis (1975), that shows an increase in  $f_w$  with increasing relative roughness k/A. More recent work by Dixen et al. (2008) has extended this result for large roughness where  $k/A \sim O(1)$ .

The dissipation of wave energy due to bed friction is associated with the component of the time varying stress that does work on the oscillatory flow. Jonsson (1966) defined the wave energy

dissipation factor  $f_e$  for sinusoidal waves based on the mean dissipation of wave energy which is given by:

$$\epsilon_{f} = \overline{\tau_{b}u_{w}\left(t\right)} = \frac{2}{3\pi}\rho f_{e}U_{w}^{3} \tag{17}$$

where  $u_w(t)$  is the time-variable freestream wave velocity. Because the bottom stress is not generally in phase with the wave motion,  $f_e$  and  $f_w$  are not strictly the same, though these are often used interchangeably. Madsen (1994) related these formally for spectral waves as a function of their corresponding phase shift.

Nielsen (1992) reviewed a number of models for turbulent wave boundary layers over homogeneous roughness. A quasi-steady model, assuming a log profile as in Equation 11, agrees reasonably well with measured velocity profiles for low relative roughness (k/A < 0.01). For large roughness (k/A > 0.06), the boundary layer structure was well-approximated using a constant eddy viscosity, consistent with wake-dominated turbulence (c.f. Pope 2000).

The extension of results for wave boundary layers for homogenous roughness to coral reefs is challenged by the broad range of coral bed morphologies. The dense canopies shown in **Figure 2** would suggest that coral reef surfaces would fall within high relative roughness values, k/A. As noted earlier, however, reef roughness is multiscaled with 'roughness elements' that also differ fundamentally from sand, gravel and rock boundaries. Though some massive corals may be well-described as solid obstacles, elements are commonly characterized at small scales by branching networks. As discussed later, the degree to which flow penetrates these elements is a function of wave frequency (Lowe et al. 2005c, Reidenbach et al. 2006) with high frequency waves tending to generate greater flow through the elements. As for steady flow, the connection between physical roughness and the associated hydrodynamic roughness used for friction factor parameterizations is thus not clear.

Reef surfaces dominated by low relief encrusting coral coverage may be well represented by homogeneous roughness wave boundary layer models. Estimates of wave dissipation factors by Lowe et al. (2005a) over a reef flat with relatively uniform, low relief roughness were well explained across a range of frequencies by a homogenous roughness parameterization using a

single roughness scale. Estimates for  $f_e$  ranged from 0.1-0.7 for frequencies between 0.1 and 0.6 Hz with higher values at higher frequencies, consistent with increasing friction and dissipation at higher relative roughness. The inferred roughness scale compared well with physical roughness measurements quantified using rms over 3 m transects. Other studies have yielded comparable estimates for dissipation factors, primarily for reef flats (Gerritsen 1981; Nelson 1996; Hearn 1999; Falter et al. 2004; Pequignet et al. 2011) and forereef environments (Gerritsen 1981; Bandet 2009; Pequignet et al. 2011; Monismith et al. 2013).

Pequignet et al. 2011 measured a higher friction factor ( $f_e$ =0.4) for a forereef in Guam with complex, multiscaled roughness, relative to the reef flat ( $f_e$ =0.06). Notably, Monismith et al. (2015) reported  $f_e$  = 1.8 for a Palmyra forereef, attributing the high dissipation to the complex canopy structure which introduces an additional component to the drag so that the wave dissipation factor, following Lowe et al. (2007), is given by:

$$f_e = f_{e_0} + C_d \lambda \alpha_w^3 \tag{18}$$

where  $f_{e0}$  is the dissipation due to drag at the bottom, with typical values of 0.01 to 0.1,  $C_d \approx 1$  is a drag coefficient associated with canopy structure,  $\lambda$  is the roughness density and  $\alpha_w$  represents the ratio of wave velocity within the canopy to the freestream wave velocity. The factor  $\alpha_w$  is dependent on wave frequency, estimated by Lowe et al. 2005b as  $0.5 < \alpha_w < 0.7$  for dense canopies and long waves.

The total stress on coral elements due to wave motion has three components: viscous shear stress, pressure drag associated with separated flow, and inertial forces (added mass effects) associated with flow acceleration. Yu et al. (2018) note that these various components of forces lead to ambiguous definitions for the wave friction factor. As discussed earlier and also shown by Yu et al. (2018), viscous shear forces are generally negligible at high Reynolds numbers characteristic of reef environments. The inertial forces on roughness elements are dominant at high wave frequencies, while pressure drag dominates for longer waves and for steady flow (Lowe et al. 2005b; Yu et al. 2018). Because the inertial forces are associated with potential flow effects, these do not contribute to the stresses that are reflected in Equation 16.

Furthermore, because these are in quadrature with the outer wave flow, inertial forces do not contribute to  $f_e$ , as evident in Equation 17.

528529

530

531

532

533

535

536

537

538

539

540

541

542

543

544

545

546

547

548

549

550

551

552

526

527

The pressure drag on the elements, associated with the second component in Equation 18, is related to vorticity formation in the wave boundary layer and is then the dominant contribution to the stress within the fluid. Using the more general Reynolds decomposition in Equation 4 to account for wave motion, it is evident that the time variable, phase-averaged vertical stress in the wave boundary layer will have two contributions:

$$\tilde{\tau}_{xz} = \rho \widetilde{u'w'} + \rho \widetilde{\tilde{u}\tilde{w}}$$
 (19)

(Nielsen 1992). Sleath (1987) showed that the second term, associated with phase-coherent turbulent motions, was dominant for flow over rough beds, relating the associated fluxes to persistent jets and bursts generated by discrete roughness elements. Bandet (2009) used alongbeam measurements from a horizontally profiling acoustic Doppler current profiler (ADCP) to resolve spatial patterns in phase-coherent motions in the outer region of the wave boundary layer over a 3m section of forereef characterized by sparse, multiscale canopy elements (Figure 3) with a red spectral roughness distribution (Nunes & Pawlak 2008). Coral roughness elements in the vicinity of the ADCP measurements extended up to 30 cm above the substrate with a rms height of  $k_{rms} = 16$  cm. Figure 3 shows phase averaged vorticity,  $\omega$  normalized by  $U_w/k_{rms}$ . The data reveal a wave boundary layer that extends up to 50 cm above the substrate but with a phase structure that varies with wave orbital amplitude. Boundary layer thickness increases slightly with orbital amplitude, but generally scales with roughness height. Single profile measurements below the roughness (not shown in Figure 3) show that the near-bed phase is invariant with increasing orbital amplitude. Changes in the vorticity phase above the roughness height arise due to increased advection from the previous cycle as the oscillatory excursions increase, reflecting influence of larger length scales as orbital amplitude increases. These variations in phase coherent vorticity thus alters the phase response for the turbulence and associated stresses in Equation 19.

553554

555

556

The near-bed orbital amplitude provides a characteristic length scale for the wave motion that can provide some guidance in determining the range of scales that are hydrodynamically relevant for wave dissipation. For a red spectral distribution, this raises an interesting scenario where

increasing orbital amplitudes statistically 'sample' larger roughness scales such that k = k(A). In this case, the ratio k/A will depend on the character of the roughness distribution.

Where roughness scales are comparable to the overall depth  $(k/h \sim O(1))$ , the wave boundary layer paradigm implicit in standard parameterizations for  $f_w$  is questionable. The drag formulation in Equation 18 may still provide a useful framework for estimating wave dissipation and boundary layer turbulence.

Wave generated turbulence near the seabed and the associated increase in momentum transfer can modify turbulence in the steady flow, increasing  $u_*$  with decreasing  $U_c/U_w$ . Grant & Madsen (1979) devised an analytical model for k << h based on a quasi-steady law of wall profile within the wave boundary layer that results in an increased 'apparent' roughness in the steady flow log profile in Equation 11. Numerous other models have been proposed using varying wave boundary layer turbulence closures for different wave-current flow regimes (c.f. Fredsoe & Deigaard 1992). Christoffersen & Jonsson (1985) used a constant eddy viscosity in the wave boundary layer applicable for large roughness. These models have not been evaluated for large multi-scale coral reef roughness.

Lentz et al. 2018 followed a simpler approach to account for wave effects on steady flow over a reef flat following the bed stress formulation considered by Wright & Thompson (1983) and Feddersen et al. (2000):

$$\tau_b = \rho C_D \overline{(\bar{\boldsymbol{u}} + \tilde{\boldsymbol{u}}) |\bar{\boldsymbol{u}} + \tilde{\boldsymbol{u}}|}$$
(20)

where the vector bed stress is determined from the time average of the instantaneous stress. This estimate for the steady stress effectively accounted for variations in  $U_c/U_w$  for a given drag coefficient or hydrodynamic roughness. Effects due to variations in the relative angle  $\phi_{wc}$  between waves and currents are included implicitly in Equation 20 since it is based on the velocity vectors. Grant & Madsen's (1979) model showed that  $\phi_{wc}$  had only small effects on the mean stress, though this has not been exhaustively verified. Equation 20 is similar to the 'linear' drag law used by Hearn (1999) where the quadratic velocity factor in Equation 9 is replaced by a steady velocity scale multiplied by a factor proportional to the wave motion.

For highly spatially variable reef topography, wave motion can drive further spatial variability in turbulence. Pawlak & MacCready (2002) showed that oscillating flow over inhomogenous roughness can drive strong residual flows, related to the periodic jets and bursts noted by Sleath (1987) in wave boundary layers. These residuals then contribute to the total near bed steady stress via the dispersive term  $\langle \bar{u}''\bar{w}'' \rangle$  in Equation 8.

# 5.0 Complications to the standard rough boundary model

It is clear that as in many inner shelf and coastal flows, the law of the wall, albeit including modifications to account for surface waves, is the fundamental model for vertical flow structure over coral reefs. Yet, there are several important aspects of these coral reef flows that can significantly affect the applicability of the law of the wall: effects of stratification, either pre-existing or due to internal waves (Davis & Monismith 2011); the effects of shallowness of the flow, i.e. the fact that the free surface can influence the largest scales of motion (Walter et al. 2011); and the effects of turbulence produced by breaking surface waves (Huang et al. 2012).

In their study of turbulence on a reef for  $h_c/h <<1$  (**Figure 2**) Davis & Monismith (2011) showed that in the absence of stratification, turbulence properties like TKE dissipation rate behaved as would be expected from the law of the wall. In contrast, in the presence of shoaling internal tides, a common feature of the field site (Leichter et al. 1996; Davis et al. 2008), stratification significantly altered the vertical structure of the flow, for example producing velocity profiles with near-bed maxima, behavior that is decidedly different from Equation 11. Accordingly, turbulence quantities like Reynolds stress profiles and TKE dissipation rate were quite different from what would be expected for the classical rough wall flow. In this case, attempts to use law of the wall velocity fits to find  $u^*$  and thus the scalar diffusivity,  $K_T$ , would be expected to be significantly in error.

Free surface effects may also significantly affect applicability of the law of the wall to coral reef flows. Firstly, while there do appear to be approaches for modeling how waves modify shallow flows (see above), there has never been an assessment of how waves model scalar fluxes. As shown in Lowe et al (2005b; 2008) wave motions in the canopy behave very differently than do mean flows in that they tend to be much less damped by drag since for waves the fundamental

force balance tends to be between accelerations and pressure gradients. One effect of this is that mass transfer in the presence of waves tends to be somewhat greater than would be expected solely on the basis of the inferred drag (Lowe et al 2005c; Falter et al. 2005). Thus, it seems unlikely that  $u_*$  inferred from log fits of flows over reefs in the presence of the waves can be used without modification to infer scalar fluxes. Secondly, it is well known that turbulence produced by breaking waves behaves quite differently from turbulence produced by bottom boundary layer drag (Terray et al 1996; Jones & Monismith 2008). Thus, given that regions of wave-breaking and thus high mass transfer (Hearn et al. 2001) may be important to overall functioning of any given reef, wave breaking may play a significant, albeit virtually unstudied, role in the overall functioning of reef ecosystems.

Finally, a subtler aspect of the presence of the free surface is its potential for modifying large-scale turbulence structures that are important to fluxes of any quantities, i.e., either of momentum or of scalars. As seen in the canonical co-spectra described by Kaimal et al. (1972), as applied to coral reefs, roughly 50% of the stress is carried by eddies with horizontal scales larger than the depth. Measurements reported by Walter et al. (2011) for tidal flow in a shallow estuary are likely similar to what might be found for shallow reef flows. They found that their co-spectra generally matched the form of the Kaimal co-spectra, differing most significantly at small wavenumbers, i.e., for scales comparable to or larger than the depth of the flow. This too may be a buoyancy effect in that large scales of turbulence in the presence of the free surface must do work against gravity to deform the free surface (e.g., Pan & Banerjee 1995). Whether or not these free surface effects are significantly large to be of practical interest in terms of influencing overall drag and mass transfer remains to be determined.

# 6.0 Within-canopy flows

Above, we have examined approaches for characterizing and quantifying structural complexity to understand its effect on the flow above the reef, but we are also interested in the structure of flow and turbulence within the 'roughness sub-layer' of the coral reef canopy as this is a chemically and biologically active region where the mass flux of material at the water-coral interface controls many important ecological processes (Section 7).

Foundational theoretical and observational work has been done in terrestrial and aquatic canopies such as forests (Belcher et al. 2012; Finnigan et al. 2009; Raupach & Thom 1981) and seagrass beds (Ghisalberti & Nepf 2002, 2006; Nepf & Vivoni 2000; Nepf 2012). These studies provide a conceptual framework for our understanding of flow in coral reef canopies. Within a canopy, flow encounters roughness elements and the forces acting on the surface of these elements dissipate kinetic energy and remove momentum from the flow. The net result of which is enhanced drag on the mean flow within the canopy. That this drag is extended over a vertical region  $(\sim h_c)$  and not just on a surface plane is what distinguishes canopy flows from more familiar boundary layer flows (Finnigan 2000). For deeply submerged or 'unconfined canopies' ( $h_c/h < 0.1$ ) of sufficient roughness density, the discontinuity in form drag between the canopy and the region above results in an inflection point in the velocity profile (Finnigan 2000; Nepf 2012). This region of strong shear produces hydrodynamic instabilities characteristic of plane mixing-layers where the turbulence is dominated by large coherent structures which transport momentum both into and away from the canopy (Raupach et al. 1996). Finnigan et al. (2009) performed large eddy simulations of canopy flow and described the nature of the turbulent structures within a vegetated canopy as pairs of linked hairpin vortices (paired sweep and ejection) between which there is a pressure maximum and, likely, a scalar microfront. The prevalence of canopy-scale coherent structures means that turbulence in canopies is far from isotropic or random and that vertical turbulent transport is an important part of the turbulent kinetic energy (TKE) balance (Raupach et al. 1996). Large coherent structures which penetrate the canopy from the free-flow region above break down quickly upon interacting with canopy elements, resulting in a spectral 'short-circuit' of turbulent energy to small wavelength structures (Finnigan 2000). Additionally, within the canopy, turbulence is created at the scale of canopy elements as flow is forced to move around branches or blades creating wakes. Within unconfined canopies the momentum balance is primarily between the shear stresses at the top of the canopy and the form drag exerted by the canopy elements (Raupach 1992). This shear-dependent momentum transfer results in a region of strong turbulence and rapid renewal of fluid from the top of the canopy down to the penetration depth of the coherent structures, but

650

651

652

653

654

655

656

657

658

659

660

661

662

663

664

665

666

667

668

669

670

671

672

673

674

675

676

677

678

679

681 below this, flow is reduced and turbulent mixing is weak (Nepf & Vivoni 2000; Ghisalberti & 682 Nepf 2006). However, when the canopy takes up a larger fraction of the total water column (0.2 683  $< h_c/h < 1$ ), such as in seagrass beds in shallow coastal waters, the external pressure gradient also 684 becomes a significant force driving flow within the canopy (Nepf 2012). The degree of canopy 685 submergence determines the relative importance of shear stresses and pressure gradient forces 686 within the canopy. As  $h_c/h$  approaches unity, the shear layer at the top of the canopy disappears 687 and flow within the canopy, driven entirely by external pressure gradients, is greater in 688 magnitude and more vertically-uniform than in unconfined canopies (Nepf & Vivoni 2000). 689 690 There are some notable differences between coral canopies and their other aquatic or terrestrial 691 counterparts. In terrestrial canopies, the flow problem is typically considered to be semi-infinite 692 or unconfined ( $h_c/h <<1$ ), but coral reefs are often in tidally-influenced and shallow coastal 693 environments and the height of the canopy can be a significant fraction of the depth of the water 694 column, even emergent at low tide, and  $h_c/h$  is time variable. Another consequence of their 695 shallow water habitats is that surface gravity waves can drive oscillatory flow within coral 696 canopies, enhancing exchange relative to uni-directional flows. Lastly, most of what we know 697 about within-canopy flows is from studies considering idealized geometry or the uniform vertical 698 and horizontal distribution of canopy roughness elements (although idealized studies of non-699 uniform roughness by Rominger & Nepf (2012) examine flow adjustments within a canopy). 700 However, the multiscale, multifractal complexity of coral reef structures results in spatially-701 variable resistance and this nonuniform structure can be important to within-canopy flow 702 structure (Duvall et al. 2019; Asher & Shavit 2019). 703 704 Observations of mean and turbulent flow structure inside realistic coral canopies are limited -705 laboratory studies (Reidenbach et al. 2007; Lowe et al. 2008, Asher et al. 2016, Asher & Shavit 706 2019) all using densely-packed arrays of coral skeletons of *Pocillopora meandrina* or *Porites* 707 compressa (both branching species) and a field study (Hench & Rosman 2013, see Figure 2f) of 708 flow around "bommies" of *Porites rus* have reported measurements on canopy flows. Of these 709 studies, Reidenbach et al. (2007) and Lowe et al. (2008) focused on comparisons of 710 unidirectional and oscillatory flow dynamics within canopies, while Hench & Rosman (2013) 711 and Asher & Shavit (2019) sought to understand role of spatially-variable canopy geometry.

712 Lowe et al. (2008) had some success adapting porous media flow theory to describe flow within 713 a relatively homogenous canopy of *Porites compressa* through the addition of a canopy shear 714 stress term. This approach characterizes the canopy resistance as a "laminar resisting force" and 715 form drag that are both dependent on a characteristic length scale of the porous medium, which 716 is assumed to be homogenous in space. However, the nonuniform spatial distribution of porosity 717 and resistance within natural coral reef canopies can generate regions of strong flow 718 accelerations, recirculation zones behind coral colonies, and interacting wakes (Hench & 719 Rosman 2013). Persistent spatial variations in flow can contribute to the "dispersive stress" term 720 that appears when the momentum equation is spatially-averaged (Equations 7 & 8). In 721 laboratory measurements of flow within a canopy of *Pocillopora meandrina* skeletons, Asher & 722 Shavit (2019) found the dispersive stress to be the dominant stress term for  $h_c/h=1$  runs, and 723 more than half of the magnitude of the Reynolds stress for  $h_c/h < 1$  cases. These results as well as 724 evidence from other studies of spatially nonuniform canopies (e.g. Bohm et al. 2013; 725 Moltchanov et al. 2015) suggest that the inner geometry of corals may generate high dispersive 726 stresses that are a significant part of the momentum balance. Furthermore, it is possible that in 727 past work, unaccounted for dispersive stresses may be responsible for observed differences 728 between bulk drag and shear stresses measured at one or a few locations near a reef boundary. 729 Further work is needed here to better understand the role of nonuniform canopy roughness in the 730 redistribution of momentum within reefs. 731 732 Reidenbach et al., (2007) carried out laboratory experiments examining the velocity and 733 turbulence structure above and within a bed of nonliving *Porites compressa* skeletons under 734 unidirectional and wave-dominated flow (Figure 4). Flow was measured with a two-735 dimensional laser Doppler anemometer and mass transport was estimated using planar laser-736 induced fluorescence (PLIF) with Rhodamine 6G dye applied to the surface of the corals. 737 Figure 4(a) is an effective visualization of the role that turbulent structures play in mass 738 transport at the coral canopy-water interface. Root-mean-square (rms) horizontal velocity  $(U_{rms} = \sqrt{\langle u^2 \rangle})$  provides a comparable velocity scale for both unidirectional and oscillatory 739 740 flows and is shown in Figure 4b. Measurements of velocity and turbulence during 741 unidirectional flow conditions (blue lines in Figure 4b,c) exhibit some features characteristic of 742 canopy flows - very weak flow within the canopy and near zero turbulent stresses (-15 cm < z < -

2 cm), an inflection point in the velocity profile at the top of the canopy and a corresponding peak in turbulent stresses (z=0), and a logarithmic velocity profile and constant stress region apparent above the canopy (1 cm < z < 6 cm). In wave-dominated runs (red lines in **Figure 4b,c**) rms horizontal velocity is still reduced within the canopy, but rms vertical velocity (not shown) is 50% higher within the canopy compared to the overlying fluid. Turbulent stresses in the wave-dominated flow peak just below the top of the canopy (z=2 cm) and are non-zero and variable throughout the canopy, especially  $\overline{w'w'}$ . A wave boundary layer of thickness,  $\delta_w=2.5$ cm was observed just above the canopy (z=0-2.5 cm). While the magnitude of the velocities in the unidirectional and oscillatory flows were similar ( $U_{rms}=9.0$ cm s<sup>-1</sup>), the increased turbulent energy in the wave-dominated run resulted in approximately twice the effective mass transfer (estimated both from PLIF analyses and using gypsum dissolution as a proxy for mass exchange) (Reidenbach et al. 2007). Some of this enhanced mass transfer is attributed to vortex ejections, identified from pulses of dye originating at the coral surface and emerging into the flow region above, which occurred repeatedly at the same phase of the wave, 150° and 270°.

# 7.0 Benthic fluxes to support ecosystem function.

- One of the primary motivations for the study of turbulent flow over and within coral reefs and other aquatic and terrestrial canopies has been to understand the physical processes governing the exchange of momentum, heat, and mass (i.e. nutrients, waste products, larvae, disease) between the fluid above and the biologically-active surface at the bed (Falter et al. 2013; Raupach & Thom 1981). Benthic marine communities, such as coral reefs, rely on the flow of
- water and turbulent mixing to sustain many biological processes, and this has been supported in

many observational studies.

In a pair of noteworthy papers, Bilger & Atkinson (1992) and Atkinson & Bilger (1992) were the first to remark the importance of turbulent mass transfer to coral reef biogeochemistry and

ecology. They were able to show that the uptake of phosphate by the reef community on the reef

flat of Kaneohe Bay, Hawaii, was "mass transfer limited," i.e., that this uptake rate was

physically controlled by turbulent mixing between the reef benthos and the overlying water

column. Mass transfer limitation is well known in the engineering literature, where, for example,

it is important to the design of heat exchangers. These studies were able to show that

experimentally determined engineering parameterizations of the flux of scalar, F, from a rough boundary, represented in terms of a mass transfer velocity,  $V_t$ , with  $F = V_t \Delta C$ , with  $\Delta C$  the concentration difference between the surface and the fluid above (e.g. Dawson & Trass 1972; Dipprey & Sabersky 1963), could be applied to the Kaneohe Bay reef. These models take the form

$$\frac{V_t}{U} = f\left(\text{Re}_h, k_s, \text{Sc}\right) \tag{21}$$

with U an appropriate mean velocity scale,  $Re_h = U h / v$  is the Reynolds number defined in terms of U and h, the outer length scale for the flow (e.g. the depth),  $k_s$  is the sand grain roughness, and Sc is the Schmidt number. However, one adjustment, an extra multiplicative factor of 6.4, was needed to fit the standard model to their reef observations. They suggested that this was because coral reefs have substantially more surface area for exchange per unit area of wall surface. Of course, one complication with this interpretation is the fact that, as shown in **Figure 5** below, there can be enormous variability in local mass transfer rates over the entire surface of a single coral colony (Chang et al. 2013).

The physics of convective mass transfer offers an explanation of the behavior seen in **Figure 5** and the parametric dependence of the mass transfer velocity. In the absence of any flows, mass transfer would take place purely by molecular diffusion, whereas in the presence of flows, there is a very thin boundary layer near the surface across which diffusion sustains a flux. The thinner this layer is, the larger the diffusive mass flux. For a flat plate or a wall, the case commonly of engineering interest, the thickness of the diffusive layer is determined by the flow away from the wall. As the velocity increases, the diffusive layer thins, and thus the mass transfer increases. However, for isolated objects, mean velocity strain can be an important determinant of local mass transfer. For example, mass transfer on a cylinder is maximal at the forward stagnation point where the velocity is zero but the compressive strain is maximal and minimal in the wake on the rear of the cylinder (Goldstein & Karni 1984; Sanitjai & Goldstein 2004; Chang et al. 2013). Thus, for a coral colony, mass transfer on parts of the colony facing into the flow are likely to be much higher than on rearward facing parts. Moreover, because of reductions of

velocity, wake interactions etc., as seen in the magnetic resonance velocimetry measurements of Chang et al (2009), mass transfer rates on the interior parts of a branching coral colony would also be much smaller than on the tips of the branches.

To examine coral colony mass transfer behavior in detail, Chang et al. (2014) carried out Large Eddy Simulations (LES) of steady and oscillating flows through four different branching corals (one of which was the coral shown in **Figure 5**). A striking finding of this work was that local mass transfer rates, including those that were wave phase dependent, were strongly correlated with the tangential component of the local wall shear stress, and not with the local pressure force, suggesting that colony-scale mass transfer might not be well parametrized by drag. Following the same approach as Chang et al. (2014), Stocking et al. (2018) used LES to study flows and mass transfer around massive (e.g. hemisphere-like) coral morphologies. They found that there could be subtle trade-offs between increasing surface area for mass transfer by increasing roughness and the concomitant reduction in local heat fluxes. These results should all be treated with some element of caution however, since: (a) both sets of calculations were done with Sc = 1 and the behavior of mass transfer for Sc >> 1 (characteristic of all scalars of interest) can differ significantly between small Sc and large Sc (Yaglom & Kader 1974); and (b) given that mass transfer is very strongly affected by the details of the near-wall flow, computed fluxes can depend on details of the calculation method and on near-wall grid resolution.

For understanding flow effects at the reef scale, what is required is knowledge of the integrated effect of the highly variable local mass transfer seen above. This was explored by Falter et al. (2016) who attempted to show how flat boundary models might be extended to include coral canopies. The starting point for this analysis is the full set of equations for drag and mass transfer given (e.g.) by Atkinson (1992). These show that generally  $V_t \propto U^{0.8}$  with a weak dependence on Sc. Falter et al. (2016) argue that the velocity dependence derived from rough wall experiments could be generalized to canopy flows by noting that the rough wall data give  $V_t \propto \tau_b^{0.4}$ , where  $\tau_b$  is the wall stress. Thus, for canopy flows, one needs to consider the effective wall stress associated with the drag on the canopy elements averaged over the entire surface (Nepf 2012). Importantly this drag and mass transfer depends on the velocity inside the canopy, which is itself a function of the free stream velocity and the canopy density and geometry. Re-analysis

of the mass transfer measurements of Lowe et al. (2005c), using as a velocity scale a hybrid velocity computed from the mean and wave velocities, showed good agreement with the  $\tau_h^{0.4}$  dependence, although this result is very much dependent on using the Reynolds number and canopy element density parametrization of Tanino & Nepf (2008) which do not account for unsteady drag effects as documented by Sarpkaya (1975). Likewise, the single colony calculations of Chang et al. (2014) suggest that the relationship between drag (primarily associated with separation and thus pressure forces) and mass transfer (associated with near-wall shear and strain) may not be robust. Nonetheless, this formalism has been used with some success to estimate mass-transfer limited nutrient fluxes on reefs other than Kaneohe Bay (Wyatt et al. 2012; Falter et al. 2012; Gruber et al. 2019). It also appears that coral bleaching may involve mass transfer limitation: Nakamura & van Woesik (2001) showed that bleaching at high water temperatures could be suppressed if flows were sufficiently strong. The mass transfer interpretation of this result relies on the possibility that bleaching is designed to prevent the build-up of oxygen produced by symbiont photosynthesis in the polyps' tissue (Lesser 1997); high rates of mass transfer may be able to enable the polyps to maintain non-harmful oxygen concentrations in their tissue. Given the strength of this result, it is surprising that few bleaching studies include flow measurements. Besides transfer of nutrients, flow and thus turbulent mixing has also been shown to be important to several other aspects of reef function: reef heterotrophy and to larval settlement. While it is known that flow can increase coral heterotrophy by increasing the supply of zooplankton to the corals (Sebens et al. 1997), flow may also increase the flux of phytoplankton and other organic material to reef organisms (Genin et al. 2009; Ribes & Atkinson 2007). Assuming law of the wall mixing (but with u\* measured directly) and using measured profiles of chlorophyll a, Monismith et al. (2010) calculated rates of phytoplankton grazing by a soft coral and sponge dominated reef in the Florida Keys, finding that grazing rates increased with increased flows and thus turbulence. A similar use of the law of the wall mixing model is also the basis for the BEAMS (Benthic Ecosystem and Acidification Measurement System) approach devised by Takeshita et al. (2016)

835

836

837

838

839

840

841

842

843

844

845

846

847

848

849

850

851

852

853

854

855

856

857

858

859

860

861

862

863

864

to measure fluxes of total alkalinity and thus the rate of net community calcification. In this approach it is assumed that (a) the eddy diffusivities of scalars ( $K_t$ ) and of momentum ( $v_t$ ) are the same; (b) that by fitting of Equation 11 to observed velocity profiles one can estimate  $u^*$ ; (c) and with  $u^*$  known,  $K_t = \kappa u_* z$ . Using these assumptions, fluxes of the scalar of interest can be estimated from profiles of scalar concentration C (c.f. Monismith et al. 2010), i.e.,

$$F = -K_t \frac{\partial C}{\partial z} \tag{22}$$

As discussed above, while logistically convenient, this approach is limited to cases where surface wave motions are minimal and where the law of the wall can be taken to be reasonably accurate, i.e., when the water column is unstratified. In the presence of stratification, vertical velocity shear can be increased because vertical mixing is suppressed by stratification (Turner 1973). In contrast, Teneva et al. (2013) estimated  $K_T$  by combining measurements of turbulence dissipation,  $\epsilon$ , and buoyancy frequency, N, with the stratified turbulence parametrization of Shih et al. (2005).

The potential effects of stratification would seem to be particularly important for reefs that experience episodic internal waves (Leichter et al. 2006; Reid et al. 2019, Wolanski & Delesalle 1995), because during internal wave events, when the water column stratification is due to the presence of internal waves (Davis & Monismith 2011), concentrations of particulates and nutrients can be substantially higher than when internal waves are not present (e.g., Leichter et al. 1996). How stratification affects mixing and turbulence is the subject of much ongoing research (see e.g. Ivey et al. 2008; Gregg et al. 2018; Monismith et al 2018) and is beyond the scope of the present review to describe in detail.

The extent to which Equation 22 can be used in the presence of surface waves is at present unknown. The fundamental challenge here is that flow behavior in the presence of waves is fundamentally different from that of steady flows. As documented by Reidenbach et al. (2007), there can be strong phase dependence of vertical mixing of scalars. Moreover, TKE production can be negative at some phases, as a result of large time varying strains associated with wave motion (Texeria & Belcher 2002). One practical effect of this behavior is that negative TKE production implies negative eddy viscosities. Given the challenges of making eddy correlation

measurements of fluxes (e.g., Long et al. 2019), it might be hoped that the time-averaged effects of this phase-dependent flow behavior may still be describable by Fickian diffusion, i.e., by an eddy diffusivity, and ideally one derivable from something like the law of the wall modified for the presence of waves (i.e. Grant & Madsen 1979)).

Consideration of the effects of turbulence on larval settlement on reefs points to the importance of aspects of coral reef turbulence other than vertical mixing. In a noteworthy laboratory study of wavy turbulent flow over a dense bed of coral skeletons (*Porites Compressa* from Kaneohe Bay), Reidenbach et al. (2009) showed that the probability of larval settlement on a reef was dependent on the detailed statistics of the near-reef velocity field produced by both turbulence and waves. The reason for this was that larval settlement requires a short period of time during which the hydrodynamic forces on the larvae are sufficiently small for the larvae to explore and attach itself to the substrate. Thus, what matters is the probability that the near-reef velocity remains sufficiently small for attachment to take place. Using measured velocities, they suggested that the probability of attachment dropped to zero for attachment times longer than about 10 sec, although given much weaker velocities inside the coral canopy itself, the probability that a larvae could successfully attach increased substantially. Extension of their results to reef structures other than densely packed *P. compressa* skeletons remains to be done.

Most of the work considering mass-transport to coral reefs has examined how aspects of the flow environment and canopy morphology act to passively modify exchange through the diffusive boundary region. However, there is some evidence that corals may be able to actively enhance mass transport using their epidermal cilia to induce counter-rotating vortices which break down the molecular diffusive region (Shapiro et al. 2014). The significance of vortical ciliary flows has not been demonstrated for a wide range of flow conditions, but could be particularly important for shaping the microenvironment at coral surfaces under very low-flow conditions within a coral canopy.

### 8.0 A turbulent future for coral reefs

The rich literature of turbulent properties in and above rough boundaries from engineering literature (as reviewed above and in Jimenez 2004, 2012) and terrestrial canopies (Raupach &

Thom 1981; Finnigan 2000; Belcher et al. 2012) benefits our understanding of turbulence and flow in coral reef habitats, but, despite the apparent similarities, some common characteristics of coral reefs make the prediction of turbulence in this environment very challenging. Bedforms and canopy roughness within natural coral reefs are inherently multiscaled and even directionally-dependent (i.e. spur-and-groove formations in Rogers et al. 2015; other examples in Reidenbach et al. 2006; Arzeno et al. 2018). There are some promising sensing technologies emerging to help quantify this complex roughness (e.g. Ferrari et al. 2016; Chirayath & Earle 2016) and we are seeing some progress in the characterization of these structures through multifractal metrics (e.g. Duvall et al. 2019). However, recent evidence suggests that the nonuniform spatial distribution of porosity and resistance elements within natural coral reefs has a significant - and in some cases, dominant - influence on the distribution of momentum within and above the coral canopy through the dispersive stress term (Asher & Shavit 2019). Waves also complicate turbulent dynamics on coral reefs. Oscillating flow over inhomogenous roughness can induce strong, spatially-varying residual flows which also contribute to dispersive stress terms. Dispersive stress is challenging to measure as it requires spatially-resolved turbulence measurements within a canopy, but its historical neglect may be responsible for the observed scatter between bulk drag estimates from flow above coral canopies and drag estimated from shear stresses only at one (or a few) points in space (noted by Rosman & Hench 2011; Lentz et al. 2017). Future work should carefully consider the influence of spatial variations on the fluxes of momentum and scalars in interpreting observations in reef environments and in applying these to numerical models. An improved understanding of turbulent processes on coral reefs is crucial for the prediction of momentum, energy, and scalar transport, as we have emphasized in this review. From an understanding of these basic fluxes, we can learn more about the physics which shape reef ecosystem processes (McClanahan et al. 2005; Nakamura & Van Woesik 2001; Nakamura et al. 2005), sediment suspension and transport (Pomeroy et al. 2015), and larval settlement on reefs (Reidenbach et al. 2009). Furthermore, we can begin to understand the physical-biological feedbacks inherent in reef ecosystems - not only how the canopy elements affect the flow and turbulent transport, but also how the physics shapes the growth and distribution of organisms within the reef canopy (see examples for other aquatic canopies in Luhar et al. 2008).

927

928

929

930

931

932

933

934

935

936

937

938

939

940

941

942

943

944

945

946

947

948

949

950

951

952

953

954

955

956

Understanding these complex feedbacks will become increasingly important if we are to effectively manage the climate-driven changes occurring in our coastal ecosystems globally. The accelerating rise in ocean temperatures has led to multiple, world-wide mass bleaching events and coral mortality in the last decade (Hughes et al. 2017). Calcifying reef organisms are the engineers of coral reef ecosystems, and thus, reduced rates of calcification and coral mortality are already resulting in system-wide changes in the architectural complexity of bed roughness and overall sea-floor elevation due to biological and mechanical erosion (Bozec et al. 2015; Yates et al. 2017). Where corals struggle to survive, turf algae can become more abundant and, in addition to competing for space and light, can alter turbulence at in the reef, reducing bed stress, which implies the reduced mass transfer of necessary metabolites (e.g. oxygen and nutrients) as well (Stocking et al. 2016). Physics is key to the recovery of these ecosystems. The dispersal of coral gametes and settling of larvae, the genetic material necessary for reef recovery or habitat redistribution, is determined by turbulence as much as by large scale currents (Reidenbach et al. 2009). Additionally, coastal managers are exploring reef restoration as a strategy to protect shorelines from erosion due to ever-higher seas (Ferrario et al. 2014). An improved understanding of drag parameterization on reefs and the influence of wave-driven turbulence would benefit this effort. **Acknowledgements:** The authors are grateful for the many collaborations and conversations that have shaped our understanding of coral reef physics through the years, notably Amatzia Genin and the late Marlin Atkinson. We'd especially like to thank Jim Hench, Ryan Lowe, Johanna Rosman, Matt Reidenbach, Uri Shavit, and Jim Falter for fruitful discussions and contributing reef images for this manuscript. K.A.D. and S.G.M. were supported in this work by the National Science Foundation (K.A.D.: OCE-1753317; SGM: OCE-1948189). G.P. would like to acknowledge support from the National Science Foundation (OCE-1829993) and the Office of Naval Research (N00014-15-2-2303).

958

959

960

961

962

963

964

965

966

967

968

969

970

971

972

973

974

975

976

977

978

979

980

981

982

983

984

985

986

- 988 **References:**
- Amador, A., Arzeno, I.B., Giddings, S.N., Merrifield, M.A., & Pawlak, G. (2020A, in review).
- 990 Cross-Shore Structure of Tidally-Driven Alongshore Flow over Rough Bathymetry. Journal of
- 991 Geophysical Research: Oceans.

- 993 Amador, A., Giddings, S.N. & Pawlak, G. (2020B, in review). ADCP-based Estimates of Lateral
- 994 Turbulent Reynolds Stresses in Wavy Coastal Environments. Limnology & Oceanography:
- 995 Methods.

996

- 997 Arzeno, I. B., Collignon, A., Merrifield, M., Giddings, S. N., & Pawlak, G. (2018). An
- 998 Alongshore Momentum Budget Over a Fringing Tropical Fore-Reef. Journal of Geophysical
- 999 Research: Oceans, 123(11), 7839-7855.

1000

- 1001 Asher, S., Niewerth, S., Koll, K., & Shavit, U. (2016). Vertical variations of coral reef drag
- forces. Journal of Geophysical Research: Oceans, 121(5), 3549-3563.

1003

- 1004 Asher, S., & Shavit, U. (2019). The effect of water depth and internal geometry on the turbulent
- flow inside a coral reef. Journal of Geophysical Research: Oceans, 124(6), 3508-3522.

1006

- Atkinson, M. J., & Bilger, R. W. (1992). Effects of water velocity on phosphate uptake in coral
- reef-hat communities. Limnology and Oceanography, 37(2), 273-279.

1009

- 1010 Atkinson, M.J. (1992). Productivity of Enewetk Atoll reef flats predicted from mass transfer
- relationships. Continental Shelf Research 12(7/8): 799-807.

1012

- Bailey, S. C., Vallikivi, M., Hultmark, M., & Smits, A. J. (2014). Estimating the value of von
- 1014 Kármán's constant in turbulent pipe flow. Journal of Fluid Mechanics, 749, 79-98.

1015

- Bandet, M., Dynamics of wave-induced boundary layers over very rough boundaries: field
- observations over a stretch of coral reef. PhD Thesis, Univ. Hawaii, 2009.

- Belcher, S. E., Harman, I. N., & Finnigan, J. J. (2012). The wind in the willows: flows in forest
- canopies in complex terrain. Annual Review of Fluid Mechanics, 44, 479-504.

- Bilger, R. W., & Atkinson, M. J. (1992). Anomalous mass transfer of phosphate on coral reef
- flats. Limnology and Oceanography, 37(2), 261-272.

1024

- Böhm, M., Finnigan, J. J., Raupach, M. R., & Hughes, D. (2013). Turbulence structure within
- and above a canopy of bluff elements. Boundary-Layer Meteorology, 146(3), 393–419.
- 1027 https://doi.org/10.1007/s10546-012-9770-1

1028

- Bozec, Y. M., Alvarez-Filip, L., & Mumby, P. J. (2015). The dynamics of architectural
- 1030 complexity on coral reefs under climate change. Global change biology, 21(1), 223-235.

1031

- Burke, L., K. Reytar, M. Spalding, and A. Perry. (2011) Reefs at Risk Revisited. Washington,
- D.C., World Resources Institute (WRI), The Nature Conservancy, WorldFish Center,
- 1034 International Coral Reef Action Network, UNEP World Conservation Monitoring Centre and
- 1035 Global Coral Reef Monitoring Network, 114p.

1036

- 1037 Chang, S., Elkins, C., Alley, M., Eaton, J., & Monismith, S. (2009). Flow inside a coral colony
- measured using magnetic resonance velocimetry. Limnology and Oceanography, 54(5), 1819-
- 1039 1827.

1040

- 1041 Chang, S., Elkins, C., Eaton, J. K., & Monismith, S. (2013). Local mass transfer measurements
- for corals and other complex geometries using gypsum dissolution. Experiments in fluids, 54(7),
- 1043 1563.

1044

- 1045 Chang, S., G. Iaccarino, F. Ham, C. Elkins, and S. Monismith (2014), Local shear and mass
- transfer on individual coral colonies: Computations in unidirectional and wave-driven flows, J.
- 1047 Geophys. Res. Oceans, 119, 2599–2619, doi:10.1002/2013JC009751.

- 1049 Chirayath, V., & Earle, S. A. (2016). Drones that see through waves–preliminary results from
- airborne fluid lensing for centimetre-scale aquatic conservation. Aquatic Conservation: Marine
- and Freshwater Ecosystems, 26, 237-250.

- 1053 Christoffersen J,.B., and I. C. Jonsson Bed friction and dissipation in a combined current and
- 1054 wave motion, Ocean Eng., 12(5), 387-423, 1985.

1055

- 1056 Claussen, M. (1990). Area-averaging of surface fluxes in a neutrally stratified, horizontally
- inhomogeneous atmospheric boundary layer. Atmospheric Environment. Part A. General Topics,
- 1058 24(6), 1349-1360

1059

- 1060 Coles, D. (1956), The law of the wake in the turbulent boundary layer, J. Fluid Mech., 1, 191–
- 1061 226, doi:10.1017/S0022112056000135.

1062

- Davis, K.A., R. Arthur, E. Reid, T.M. DeCarlo, and A. Cohen. (2020) Fate of internal waves on
- a shallow shelf. *Journal of Geophysical Research Oceans, DOI:* 10.1029/2019JC015377.

1065

- Davis, K. A., Leichter, J. J., Hench, J. L., & Monismith, S. G. (2008). Effects of western
- boundary current dynamics on the internal wave field of the Southeast Florida shelf. Journal of
- 1068 Geophysical Research: Oceans, 113(C9).

1069

- Davis, K. A., & Monismith, S. G. (2011). The modification of bottom boundary layer turbulence
- and mixing by internal waves shoaling on a barrier reef. Journal of Physical Oceanography,
- 1072 41(11), 2223-2241.

1073

- Dawson DA, Trass O. 1972. Mass transfer at rough surfaces. Int. J. Heat Mass Trans. 15:1317–
- 1075 36.

1076

- D'elia, C. F., & Wiebe, W. J. (1990). Biogeochemical nutrient cycles in coral-reef ecosystems.
- 1078 *Ecosystems of the world*, *25*, 49-74.

- Dipprey DF, Sabersky RH. 1963. Heat and momentum transfer in smooth and rough tubes at
- various Prandtl numbers. Int. J. Heat Mass Trans. 6:329–53

- Dixen, M., Hatipoglu, F., Sumer, B. M., & Fredsøe, J. (2008). Wave boundary layer over a
- stone-covered bed. Coastal Engineering, 55(1), 1-20.

1085

- Duvall, M. S., Hench, J. L., & Rosman, J. H. (2019). Collapsing complexity: quantifying
- multiscale properties of reef topography. Journal of Geophysical Research: Oceans, 124(7),
- 1088 5021-5038.

1089

- 1090 Dvorak, F. A., 1969, "Calculation of Turbulent Boundary Layers on Rough Surfaces in Pressure
- 1091 Gradients," AIAA J., 7, pp. 1752–1759.

1092

- Falter JL, Atkinson MJ, Merrifield M. 2004. Mass-transfer limitation of nutrient uptake by a
- wave-dominated reef flat community. Limnol. Oceanog. 49:1820–31.

1095

- Falter, J. L., Atkinson, M. J., & Coimbra, C. F. (2005). Effects of surface roughness and
- oscillatory flow on the dissolution of plaster forms: Evidence for nutrient mass transfer to coral
- reef communities. Limnology and oceanography, 50(1), 246-254.

1099

- Falter, J. L., Atkinson, M. J., Lowe, R. J., Monismith, S. G., & Koseff, J. R. (2007). Effects of
- nonlocal turbulence on the mass transfer of dissolved species to reef corals. Limnology and
- oceanography, 52(1), 274-285.

1103

- Falter, J. L., Lowe, R. J., Atkinson, M. J., & Cuet, P. (2012). Seasonal coupling and de-coupling
- of net calcification rates from coral reef metabolism and carbonate chemistry at Ningaloo Reef,
- Western Australia. Journal of Geophysical Research: Oceans, 117(C5).

- Falter, J. L., Lowe, R. J., Zhang, Z., & McCulloch, M. (2013). Physical and biological controls
- on the carbonate chemistry of coral reef waters: effects of metabolism, wave forcing, sea level,
- and geomorphology. PloS one, 8(1).

- 1111
- Falter, J. L., Lowe, R. J., & Zhang, Z. (2016). Toward a universal mass-momentum transfer
- relationship for predicting nutrient uptake and metabolite exchange in benthic reef communities.
- Geophysical Research Letters, 43(18), 9764-9772.
- 1115
- Feddersen, F., Guza, R. T., Elgar, S., & Herbers, T. H. C. (2000). Velocity moments in
- alongshore bottom stress parameterizations. *Journal of Geophysical Research: Oceans*, 105(C4),
- 1118 8673-8686.
- 1119
- Ferrari, R., McKinnon, D., He, H., Smith, R. N., Corke, P., González-Rivero, M., ... & Upcroft,
- B. (2016). Quantifying multiscale habitat structural complexity: a cost-effective framework for
- underwater 3D modelling. Remote Sensing, 8(2), 113.
- 1123
- Ferrario, F., Beck, M., Storlazzi, C., Micheli, F., Shepard, C., Airoldi, L. (2014). The
- effectiveness of coral reefs for coastal hazard risk reduction and adaptation. *Nat Commun* 5,
- 1126 3794.
- 1127
- Finnigan, J. (2000). Turbulence in plant canopies. Annual review of fluid mechanics, 32(1), 519-
- 1129 571.
- 1130
- Finnigan, J. J., Shaw, R. H., & Patton, E. G. (2009). Turbulence structure above a vegetation
- canopy. Journal of Fluid Mechanics, 637, 387-424.
- 1133
- Flack, K.A. and Schultz, M.P., 2010. Review of hydraulic roughness scales in the fully rough
- regime. Journal of Fluids Engineering, 132(4).
- 1136
- Fredsøe, J., & Deigaard, R. (1992). Mechanics of coastal sediment transport (Vol. 3, p. 369).
- 1138 Singapore: World scientific.
- 1139
- Gerritsen F (1981) Wave attenuation and wave set-up on a coastal reef. Technical report. Look
- 1141 Lab, Univ. Hawaii, Honolulu

- Genin, A., Monismith, S. G., Reidenbach, M. A., Yahel, G., & Koseff, J. R. (2009). Intense
- benthic grazing of phytoplankton in a coral reef. Limnology and Oceanography, 54(3), 938-951.

1145

- Ghisalberti, M., & Nepf, H. M. (2002). Mixing layers and coherent structures in vegetated
- aguatic flows. Journal of Geophysical Research: Oceans, 107(C2), 3-1.

1148

- Ghisalberti, M., & Nepf, H. (2006). The structure of the shear layer in flows over rigid and
- flexible canopies. Environmental Fluid Mechanics, 6(3), 277-301.

1151

- Goldstein, R. J., and Kami, J., 1984, "The Effect of a Wall Boundary-Layer on Local Mass
- 1153 Transfer From a Cylinder in Crossflow," ASME Journal of Heat Transfer, Vol. 106, pp. 260-267.

1154

- Graham, N. A. J., & Nash, K. L. (2013). The importance of structural complexity in coral reef
- ecosystems. Coral Reefs, 32(2), 315-326

1157

- 1158 Grant, W. D., and O. S. Madsen, 1979: Combined wave and current interaction with a rough
- bottom. Journal of Geophysical Research (Oceans), 84, 1797–1807,
- 1160 https://doi.org/10.1029/JC084iC04p01797.

1161

- Grant, W.D., O.S. Madsen (1986) The continental shelf bottom boundary layer, Annual Review
- of Fluid Mechanics (M. Van Dyke, ed.), 18:265-305.

1164

- Gratwicke B, Speight MR. Effects of habitat complexity on Caribbean marine fish assemblages.
- 1166 Marine Ecology-Progress Series. 2005; 292: 301-310.

1167

- Green, A. (2002) "Status of coral reefs on the main volcanic islands of American Samoa: a
- resurvey of long term monitoring sites (benthic communities, fish communities, and key
- macroinvertebrates)." Report of the Department and Marine and Wildlife Resources, Pago Pago,
- 1171 American Samoa.

- Gregg, M.C., E.A. D'Asaro, J.J. Riley and E. Kunze, (2018), Mixing efficiency in the ocean,
- 1174 Annual Reviews of Marine Science, 10, 9.1–9.31.

- Gruber, R. K., Lowe, R. J., & Falter, J. L. (2019). Tidal and seasonal forcing of dissolved
- nutrient fluxes in reef communities. Biogeosciences, 16(9).

1178

- Guo, J., & Julien, P. Y. (2006). Application of modified log-wake law in open-channels. In
- World Environmental and Water Resource Congress 2006: Examining the Confluence of
- 1181 Environmental and Water Concerns (pp. 1-9).

1182

- Harborne AR, Mumby PJ, Ferrari R (2012) The effectiveness of different meso-scale rugosity
- metrics for predicting intra-habitat variation in coral-reef fish assemblages. Environ Biol Fish
- 1185 94:431–442

1186

- Hearn, C. J. (1999), Wave-breaking hydrodynamics within coral reef systems and the effect of
- 1188 changing relative sea level, J. Geophys. Res., 104(C12), 30,007–30,019,
- 1189 doi:10.1029/1999JC900262.

1190

- Hearn, C., Atkinson, M., & Falter, J. (2001). A physical derivation of nutrient-uptake rates in
- 1192 coral reefs: effects of roughness and waves. Coral Reefs, 20(4), 347-356.

1193

- Heathershaw, A. D., and J. H. Simpson, 1978. The sampling variability of the Reynolds stress
- and its relation to boundary shear stress and drag coefficient measurements. Estuar. Coast. Shelf
- 1196 Sci. 6: 263–274

1197

- Hench, J. L., & Rosman, J. H. (2013). Observations of spatial flow patterns at the coral colony
- scale on a shallow reef flat. Journal of Geophysical Research: Oceans, 118(3), 1142-1156.

- Holbrook SJ, Brooks AJ, Schmitt RJ (2002) Variation in structural attributes of patch-forming
- 1202 corals and in patterns of abundance of associated fishes. Mar Freshw Res 53:1045–1053
- Howard KG, Schumacher BD, Parrish JD (2009)

- 1204
- Huang, Z. C., Lenain, L., Melville, W. K., Middleton, J. H., Reineman, B., Statom, N., &
- McCabe, R. M. (2012). Dissipation of wave energy and turbulence in a shallow coral reef
- lagoon. Journal of Geophysical Research: Oceans, 117(C3).
- 1208
- Hughes, T. P. et al. Global warming and recurrent mass bleaching of corals. Nature 543, 373–
- 1210 377 (2017).
- 1211
- 1212 Ivey, G.N., K.B. Winters, and J.R. Koseff, 2008: Density stratification, turbulence, but how
- much mixing? Annual Review of Fluid Mechanics 40, 169-184.
- 1214
- Jackson, P. S. "On the displacement height in the logarithmic velocity profile." Journal of Fluid
- 1216 Mechanics 111 (1981): 15-25.
- 1217
- Jaramillo, S., & Pawlak, G. (2011). AUV-based bed roughness mapping over a tropical reef.
- 1219 Coral Reefs, 30(1), 11-23.
- 1220
- Jiménez, J. (2004). Turbulent flows over rough walls. Annu. Rev. Fluid Mech., 36, 173-196.
- 1222
- 1223 Jiménez, J. (2012). Cascades in wall-bounded turbulence. Annual Review of Fluid Mechanics,
- 1224 44, 27-45.
- 1225
- Jones, N. L., & Monismith, S. G. (2008). The influence of whitecapping waves on the vertical
- structure of turbulence in a shallow estuarine embayment. Journal of Physical Oceanography,
- 1228 38(7), 1563-1580.
- 1229
- Jonsson, I. G. (1967). Wave boundary layers and friction factors. In Coastal Engineering 1966
- 1231 (pp. 127-148).
- 1232
- Kaimal JC, Wyngaard JC, Izumi Y, Cote OR. 1972. Spectral characteristics of surface layer
- 1234 turbulence. Q. J. R. Meteorol. Soc. 98:563–89

- Kamphuis, J. W. (1975). Friction factor under oscillatory waves. *Journal of the Waterways*,
- 1237 *Harbors and Coastal Engineering Division*, 101(2), 135-144.

1238

- Koehl M.A.R., Strother J.A., Reidenbach M.A., Koseff J.R., and Hadfield M.G., 2007,
- 1240 Individual-based model of larval transport to coral reefs in turbulent, wave-driven flow:
- behavioral responses to dissolved settlement inducer, Marine Ecology Progress Series, 335, 1-
- 1242 18.

1243

- Leichter, J. J., Wing, S. R., Miller, S. L., & Denny, M. W. (1996). Pulsed delivery of
- subthermocline water to Conch Reef (Florida Keys) by internal tidal bores. Limnology and
- 1246 Oceanography, 41(7), 1490-1501.

1247

- Lentz, S.J., J.H. Churchill, K.A. Davis, J.T. Farrar, J. Pineda, and V. Starczak. (2016) The
- characteristics and dynamics of wave-driven flow across a platform coral reef in the Red Sea.
- 1250 Journal of Geophysical Research: Oceans, 121(2), 1360-1376.

1251

- Lentz, S. J., Davis, K. A., Churchill, J. H., & DeCarlo, T. M. (2017). Coral reef drag
- 1253 coefficients—water depth dependence. *Journal of Physical Oceanography*, 47(5), 1061-1075.

1254

- Lentz, S. J., Churchill, J. H., & Davis, K. A. (2018). Coral reef drag coefficients—Surface
- gravity wave enhancement. Journal of Physical Oceanography, 48(7), 1555-1566.

1257

- Leonardi, S., Paolo Orlandi, R. J. Smalley, L. Djenidi, and R. A. Antonia. "Direct numerical
- simulations of turbulent channel flow with transverse square bars on one wall." *Journal of Fluid*
- 1260 *Mechanics* 491 (2003): 229-238.

1261

- Lesser, M. P. (1997). Oxidative stress causes coral bleaching during exposure to elevated
- 1263 temperatures. Coral reefs, 16(3), 187-192.

- Long, C.E., Wiberg, P.L. and Nowell, A.R., 1993. Evaluation of von Karman's constant from
- integral flow parameters. Journal of Hydraulic Engineering, 119(10), pp.1182-1190.

- Long, M.H., J. E. Rheuban, D. C. McCorkle, D. J. Burdige, and R. C. Zimmerman 2019. Closing
- the oxygen mass balance in shallow coastal ecosystems. Limnology and Oceanography, 64,
- 1270 2694–2708.

1271

- Lowe, R. J., & Falter, J. L. (2015). Oceanic forcing of coral reefs. Annual review of marine
- 1273 science, 7, 43-66.

1274

- Lowe, R. J., Falter, J. L., Bandet, M. D., Pawlak, G., Atkinson, M. J., Monismith, S. G., &
- Koseff, J. R. (2005a). Spectral wave dissipation over a barrier reef. Journal of Geophysical
- 1277 Research, 110, C04001. https://doi.org/10.1029/2004JC002711

1278

- Lowe, R. J., J. R. Koseff, and S. G. Monismith (2005b), Oscillatory flow through submerged
- canopies: 1. Velocity structure, J. Geophys. Res., 110, C10016, doi:10.1029/2004JC002788.

1281

- Lowe, R. J., Koseff, J. R., Monismith, S. G., & Falter, J. L. (2005c). Oscillatory flow through
- submerged canopies: 2. Canopy mass transfer. Journal of Geophysical Research: Oceans,
- 1284 110(C10).

1285

- Lowe, R. J., Falter, J. L., Koseff, J. R., Monismith, S. G., & Atkinson, M. J. (2007). Spectral
- wave flow attenuation within submerged canopies: Implications for wave energy dissipation.
- 1288 Journal of Geophysical Research: Oceans, 112(C5).

1289

- Lowe, R. J., Shavit, U., Falter, J. L., Koseff, J. R., & Monismith, S. G. (2008). Modeling flow in
- 1291 coral communities with and without waves: A synthesis of porous media and canopy flow
- approaches. Limnology and Oceanography, 53(6), 2668-2680.

- Lueck, R. G., & Lu, Y. (1997). The logarithmic layer in a tidal channel. Continental Shelf
- 1295 Research, 17(14), 1785-1801.

- 1296
- Lugo-Fernandez A, Roberts HH, Wiseman WJ, Carter BL. 1998. Water level and currents of
- tidal and infragravity periods at Tague Reef, St. Croix (USVI). Coral Reefs 17:343–49
- 1299
- Luhar, Mitul, Jeffery Rominger, & Heidi Nepf (2008). Interaction between flow, transport, and
- vegetation spatial structure. Environ. Fluid. Mech, 8, 423-439.
- 1302
- 1303 Madsen, O. S. (1994), Spectral wave-current bottom boundary layer flows, in Coastal
- Engineering 1994: Proceedings of the Twenty-Fourth Inter- national Conference, edited by B. L.
- 1305 Edge, pp. 623–634, Am. Soc. of Civ. Eng., Reston, Va.
- 1306
- 1307 Mahrt, L. (1987). Grid-averaged surface fluxes. Monthly weather review, 115(8), 1550-1560.
- 1308
- Mahrt, L. (2000). Surface heterogeneity and vertical structure of the boundary layer. Boundary-
- 1310 Layer Meteorology, 96(1-2), 33-62.
- 1311
- Mason, P. J.: 1988, 'The Formation of Areally Averaged Roughness Lengths', Quart. J. Roy.
- 1313 Meteorol. Soc. 114, 399–420.
- 1314
- McClanahan, T. R., Maina, J., Moothien-Pillay, R., & Baker, A. C. (2005). Effects of
- geography, taxa, water flow, and temperature variation on coral bleaching intensity in
- Mauritius. Marine Ecology Progress Series, 71(1), 130–134.
- 1318 https://doi.org/10.1016/j.cryobiol.2015.04.009
- 1319
- McDonald, C. B., Koseff, J. R., & Monismith, S. G. (2006). Effects of the depth to coral height
- ratio on drag coefficients for unidirectional flow over coral. Limnology and oceanography,
- 1322 51(3), 1294-1301.
- 1323
- Moltchanov, S., Bohbot-Raviv, Y., Duman, T., & Shavit, U. (2015). Canopy edge flow: A
- momentum balance analysis. Water Resources Research, 51, 2081–2095.
- 1326 https://doi.org/10.1002/2014WR015397

- 1327
- Molina, L., Pawlak, G., Wells, J. R., Monismith, S. G., & Merrifield, M. A. (2014). Diurnal
- 1329 cross-shore thermal exchange on a tropical forereef. Journal of Geophysical Research: Oceans,
- 1330 119(9), 6101-6120.
- 1331
- Monismith, S. G., Genin, A., Reidenbach, M. A., Yahel, G., & Koseff, J. R. (2006). Thermally
- driven exchanges between a coral reef and the adjoining ocean. Journal of Physical
- 1334 Oceanography, 36(7), 1332-1347.
- 1335
- Monismith, S. G. (2007). Hydrodynamics of coral reefs. Annu. Rev. Fluid Mech., 39, 37-55.
- 1337
- Monismith, S. G., Davis, K. A., Shellenbarger, G. G., Hench, J. L., Nidzieko, N. J., Santoro, A.
- 1339 E., ... & Lindquist, N. L. (2010). Flow effects on benthic grazing on phytoplankton by a
- 1340 Caribbean reef. Limnology and Oceanography, 55(5), 1881-1892.
- 1341
- Monismith, S. G., Herdman, L. M., Ahmerkamp, S., & Hench, J. L. (2013). Wave
- transformation and wave-driven flow across a steep coral reef. Journal of Physical
- 1344 Oceanography, 43(7), 1356-1379.
- Monismith, S. G., Rogers, J. S., Koweek, D., & Dunbar, R. B. (2015). Frictional wave
- dissipation on a remarkably rough reef. Geophysical Research Letters, 42(10), 4063-4071.
- Monismith, S.G., J.R. Koseff, and B.L. White 2018. Mixing efficiency in the presence of
- stratification: Is it constant? Geophysical Research Letters, 45(11), 5627-5634.
- Nakamura, T., & Van Woesik, R. (2001). Water-flow rates and passive diffusion partially
- explain differential survival of corals during the 1998 bleaching event. Marine Ecology Progress
- 1351 Series, 212(2), 301–304.
- Nakamura, T., Van Woesik, R., & Yamasaki, H. (2005). Photoinhibition of photosynthesis is
- reduced by water flow in the reef-building coral Acropora digitifera. Marine Ecology Progress
- 1354 Series, 301, 109–118. https://doi.org/10.3354/meps301109

- Napoli, E., V. Armenio, and M. DeMarchis, (2008). The effect of the slope of irregularly
- distributed roughness elements on turbulent wall-bounded flows, J. Fluid Mech. 613, 385–394.

- Nelson, R. C. (1996). Hydraulic roughness of coral reef platforms. Applied Ocean Research,
- 1359 18(5), 265-274.

1360

- Nepf, H. M., & Vivoni, E. R. (2000). Flow structure in depth-limited, vegetated flow. Journal of
- 1362 Geophysical Research: Oceans, 105(C12), 28547-28557.

1363

- Nepf, H. M. (2012). Flow and transport in regions with aquatic vegetation. Annual review of
- 1365 fluid mechanics, 44, 123-142.

1366

Nezu, I., and H. Nakagawa, 1993: Turbulence in Open-Channel Flows. A. A. Balkema, 281 pp.

1368

- Nielsen, P. (1992). Coastal bottom boundary layers and sediment transport (Vol. 4). World
- scientific.

1371

- Nikuradse J (1933), Stromungsgesetze in rauhen Rohren, Forschungshefte, 361,
- 1373 VDI; NACA Tech Mem 1292.

1374

- Nunes, V., & Pawlak, G. (2008). Observations of bed roughness of a coral reef. Journal of
- 1376 Coastal Research, 39-50.

1377

- Pan, Y. & Banerjee, S. (1995) A numerical study of free-surface turbulence in channel flow.
- 1379 Phys. Fluids 7:1649-1664.

1380

- Pawlak, G., & MacCready, P. (2002). Oscillatory flow across an irregular boundary. Journal of
- 1382 Geophysical Research: Oceans, 107(C5), 4-1.

- Perry, A. E., Schofield, W. H., & Joubert, P. N. (1969). Rough wall turbulent boundary layers.
- 1385 *Journal of Fluid Mechanics*, *37*(2), 383-413.

- 1386
- Péquignet, A.-C., J. M. Becker, M. A. Merrifield, and S. J. Boc, 2011: The dissipation of wind
- wave energy across a fringing reef at Ipan, Guam. Coral Reefs, 30 (Suppl.), 71–82,
- 1389 https://doi.org/10.1007/s00338-011-0719-5.
- 1390
- Pomeroy, A., Lowe, R., Symonds, G., Van Dongeren, A., & Moore, C. (2012). The dynamics of
- infragravity wave transformation over a fringing reef. Journal of Geophysical Research: Oceans,
- 1393 117(C11).
- 1394
- Pomeroy, A. W., Lowe, R. J., Van Dongeren, A. R., Ghisalberti, M., Bodde, W., & Roelvink, D.
- 1396 (2015). Spectral wave-driven sediment transport across a fringing reef. Coastal Engineering, 98,
- 1397 78-94.
- 1398
- Pope, S. B. (2000), Turbulent Flows, 771 pp., Cambridge Univ. Press, Cambridge, U. K.
- 1400
- Rajagopalan, K., "Large eddy simulation of turbulent boundary layers over rough bathymetry",
- 1402 PhD Thesis, Univ. Hawaii, 2010
- 1403
- Raupach, M. (1992). Drag and drag partition on rough surfaces. *Boundary-Layer Meteorology*,
- 1405 *60*(4), 375-395.
- 1406
- Raupach, M. R., & Thom, A. S. (1981). Turbulence in and above plant canopies. Annual Review
- 1408 of Fluid Mechanics, 13(1), 97-129.
- 1409
- Raupach M, Shaw R. 1982. Averaging procedures for flow within vegetation canopies. Bound.-
- 1411 Layer Meteorol. 22:79–90
- 1412
- Raupach, M. R., R. A. Antonia, and S. Rajagopalan. "Rough-wall turbulent boundary layers."
- 1414 (1991): 1-25.
- 1415

- Raupach, M., Finnigan, J. J., & Brunet, Y. (1996). Coherent eddies and turbulence in vegetation
- canopies: the mixing-layer analogy. In Boundary-layer meteorology 25th anniversary volume,
- 1418 1970–1995 (pp. 351-382). Springer, Dordrecht.

- Reid, E. C., DeCarlo, T. M., Cohen, A. L., Wong, G. T., Lentz, S. J., Safaie, A., ... & Davis, K.
- 1421 A. (2019). Internal waves influence the thermal and nutrient environment on a shallow coral reef.
- 1422 Limnology and Oceanography, 64(5), 1949-1965.

1423

- Reidenbach, M. A., Monismith, S. G., Koseff, J. R., Yahel, G., & Genin, A. (2006). Boundary
- layer turbulence and flow structure over a fringing coral reef. Limnology and oceanography,
- 1426 51(5), 1956-1968.

1427

- Reidenbach M.A., Koseff J.R., and Monismith S.G., 2007, Laboratory experiments of fine-scale
- mixing and mass transport within a coral canopy, *Physics of Fluids*, 19(7), 075107,
- 1430 doi:10.1063/1.2752189.

1431

- Reidenbach, M. A., Koseff, J. R., & Koehl, M. A. R. (2009). Hydrodynamic forces on larvae
- affect their settlement on coral reefs in turbulent, wave-driven flow. Limnology and
- 1434 Oceanography, 54(1), 318-330.

1435

- Ribes, M., and M. J. Atkinson. 2007. Effects of water velocity on picoplankton uptake by coral
- reef communities. Coral Reefs **26**: 413-421.

1438

- Risk, M. J. 1972. "Fish diversity on a coral reef in the Virgin Islands." *Atoll Res. Bull.* 193:1-6
- 1440 [doi:10.5479/si.00775630.153.1]

1441

- Rogers, J. S., Monismith, S. G., Dunbar, R. B., & Koweek, D. (2015). Field observations of
- wave-driven circulation over spur and groove formations on a coral reef. Journal of Geophysical
- 1444 Research: Oceans, 120(1), 145-160.

- Rogers, J. S., Maticka, S. A., Chirayath, V., Woodson, C. B., Alonso, J. J., & Monismith, S. G.
- 1447 (2018). Connecting flow over complex terrain to hydrodynamic roughness on a coral reef.
- Journal of Physical Oceanography, 48(7), 1567-1587.

- Rominger, J. T., & Nepf, H. M. (2011). Flow adjustment and interior flow associated with a
- rectangular porous obstruction. Journal of Fluid Mechanics, 680, 636-659.

1452

- Rosman, J. H., & Hench, J. L. (2011). A framework for understanding drag parameterizations for
- 1454 coral reefs. Journal of Geophysical Research: Oceans, 116(C8).

1455

- Sanford, T. B., & Lien, R. C. (1999). Turbulent properties in a homogeneous tidal bottom
- boundary layer. Journal of Geophysical Research: Oceans, 104(C1), 1245-1257.

1458

- Sanitjai, S. and R.J. Goldstein 2004. Heat transfer from a circular cylinder to mixtures of
- water and ethylene glycol, International Journal of Heat and Mass Transfer 47 4785–4794

1461

- Sarpkaya, T. (1975). Forces on cylinders and spheres in a sinusoidally oscillating fluid. J. Appl.
- 1463 Mech. Mar 1975, 42(1): 32-37

1464

- 1465 Schlichting, H. (1937). Experimental investigation of the problem of surface roughness, NACA
- 1466 TM 823.

1467

- 1468 Schultz, M. P., and Flack, K. A., 2009, "Turbulent Boundary Layers on a Systematically-Varied
- 1469 Rough Wall," Phys. Fluids, 21, p. 015104.

1470

- Sebens KP, Witting J, Helmuth BST (1997) Effects of water flow and branch spacing on particle
- capture by the reef coral Madracis mirabilis (Duchassaing and Michelotti). J Exp Mar Biol Ecol
- 1473 211:1–28

- 1475 Sebens KP, Grace SP, Helmuth B, Maney EJ, Miles JS. 1998. Water flow and prey capture by
- three scleractinian corals, Madracis mirabilis, Montastrea cavernosa and Porites porites, in a field
- 1477 enclosure. Mar. Biol. 131:347–60

- 1479 Sebens, K. P., Helmuth, B., Carrington, E., & Agius, B. (2003). Effects of water flow on growth
- and energetics of the scleractinian coral Agaricia tenuifolia in Belize. Coral reefs, 22(1), 35-47.

1481

- Shapiro, O. H., Fernandez, V. I., Garren, M., Guasto, J. S., Debaillon-Vesque, F. P., Kramarsky-
- 1483 Winter, E., ... & Stocker, R. (2014). Vortical ciliary flows actively enhance mass transport in reef
- 1484 corals. Proceedings of the National Academy of Sciences, 111(37), 13391-13396.

1485

- 1486 Shih, L. H., Koseff, J. R., Ivey, G. N., & Ferziger, J. H. (2005). Parameterization of turbulent
- fluxes and scales using homogeneous sheared stably stratified turbulence simulations. Journal of
- 1488 Fluid Mechanics, 525, 193-214.

1489

- 1490 Sigal, A., & Danberg, J. E. (1990). New correlation of roughness density effect on the turbulent
- 1491 boundary layer. AIAA journal, 28(3), 554-556.

1492

- 1493 Sleath, J. F. A. (1987). Turbulent oscillatory flow over rough beds. Journal of Fluid Mechanics,
- 1494 182, 369-409.

1495

- 1496 Stacey, M. T., Monismith, S. G., & Burau, J. R. (1999). Measurements of Reynolds stress
- profiles in unstratified tidal flow. Journal of Geophysical Research: Oceans, 104(C5), 10933-
- 1498 10949.

1499

- 1500 Stocking, J. B., Rippe, J. P., & Reidenbach, M. A. (2016). Structure and dynamics of turbulent
- boundary layer flow over healthy and algae-covered corals. Coral Reefs, 35(3), 1047-1059.

- 1503 Stocking JB, Laforsch C, Sigl R, Reidenbach MA. 2018. The role of turbulent hydrodynamics
- and surface morphology on heat and mass transfer in corals. J. R. Soc. Interface 15: 20180448.
- 1505 http://dx.doi.org/10.1098/rsif.2018.0448

- 1506
- 1507 Storlazzi, C., J. Logan, and M. Field (2003), Quantitative morphology of a fringing reef tract
- 1508 from high-resolution laser bathymetry: Southern Molokai, Hawaii, Geol. Soc. Am. Bull.,
- 1509 115(11), 1344–1355, doi:10.1130/B25200.1.

- 1511 Swart D (1974) Offshore sediment transport and equilibrium beach profiles. Technical report
- 1512 131, Delft Hydraulic Laboratory, Netherlands.
- Taebi, S., Lowe, R. J., Pattiaratchi, C. B., Ivey, G. N., Symonds, G., & Brinkman, R. (2011).
- Nearshore circulation in a tropical fringing reef system. Journal of Geophysical Research:
- 1515 Oceans, 116(C2).
- Takeshita, Y., McGillis, W., Briggs, E. M., Carter, A. L., Donham, E. M., Martz, T. R., ... &
- 1517 Smith, J. E. (2016). Assessment of net community production and calcification of a coral reef
- using a boundary layer approach. Journal of Geophysical Research: Oceans, 121(8), 5655-5671.
- Talke, S. A., Horner-Devine, A. R., Chickadel, C. C., & Jessup, A. T. (2013). Turbulent kinetic
- energy and coherent structures in a tidal river. Journal of Geophysical Research: Oceans,
- 1521 118(12), 6965-6981.
- Tanino, Y., & Nepf, H. M. (2008). Laboratory investigation of mean drag in a random array of
- rigid, emergent cylinders. Journal of Hydraulic Engineering, 134(1), 34-41.
- Taylor, P. A. (1987). Comments and further analysis on effective roughness lengths for use in
- numerical three-dimensional models. Boundary-Layer Meteorology, 39(4), 403-418.
- 1526 Teixeira MAC, Belcher SE. 2002. On the distribution of turbulence by a progressive surface
- 1527 wave. J. Fluid Mech. 458:229–67
- 1528 Terray, E. A., M. A. Donelan, Y. C. Agrawal, W. M. Drennan, K. K. Kahma, A. J. Williams, P.
- 1529 A. Hwang, and S. A. Kitaigorodskii 1996. Estimates of kinetic energy dissipation under breaking
- 1530 waves. J. Phys. Oceanogr., 26: 792–807.

- 1532 Teneva, L., Dunbar, R. B., Mucciarone, D. A., Dunckley, J. F., & Koseff, J. R. (2013). High-
- resolution carbon budgets on a Palau back-reef modulated by interactions between
- hydrodynamics and reef metabolism. Limnology and oceanography, 58(5), 1851-1870.
- 1535 Thomas FIM, Atkinson MJ. 1997. Ammonium uptake by coral reefs: effects of water velocity
- and surface roughness on mass transfer. Limnol. Oceanogr. 42:81–88
- 1537 Trowbridge, J. H., & Lentz, S. J. (2018). The bottom boundary layer. Annual Review of Marine
- 1538 Science, 10, 397-420.

Turner, J. S. (1973). Buoyancy effects in fluids. Cambridge university press.

1541

- 1542 Veron, J. E. N. (1995). Corals in space and time: the biogeography and evolution of the
- 1543 Scleractinia. Cornell University Press.

1544

- 1545 Van Rij, J. A., Belnap, B. J., & Ligrani, P. M. (2002). Analysis and experiments on three-
- dimensional, irregular surface roughness. J. Fluids Eng., 124(3), 671-677.

1547

- Walter, R. K., Nidzieko, N. J., & Monismith, S. G. (2011). Similarity scaling of turbulence
- spectra and cospectra in a shallow tidal flow. Journal of Geophysical Research: Oceans,
- 1550 116(C10).

1551

- Wolanski, E., & Delesalle, B. (1995). Upwelling by internal waves, Tahiti, French Polynesia.
- 1553 *Continental shelf research*, *15*(2-3), 357-368.

1554

- Wooding R A, Bradley E F, and Marshall J K (1973), Drag due to regular arrays of roughness
- elements of varying geometry, *Boundary-Layer Meteorol* 5, 285-308.

1557

- Wright, D. G., & Thompson, K. R. (1983). Time-averaged forms of the nonlinear stress law.
- Journal of Physical Oceanography, 13(2), 341-345.

- Wyatt, A. S., Falter, J. L., Lowe, R. J., Humphries, S., & Waite, A. M. (2012). Oceanographic
- 1562 forcing of nutrient uptake and release over a fringing coral reef. Limnology and Oceanography,
- 1563 57(2), 401-419.

- 1565 Yates, K. K., Zawada, D. G., Smiley, N. A., & Tiling-Range, G. (2017). Divergence of seafloor
- elevation and sea level rise in coral reef ecosystems. *Biogeosciences*, 14(6), 1739.

1567

- 1568 Yaglom, A. M. & Kader, B. A. 1974 Heat and mass transfer between a rough wall and turbulent
- 1569 fluid flow at high Reynolds and Péclet numbers. J. Fluid Mech. **62**, 601–623.

1570

- 1571 Yu, X., Rosman, J. H., & Hench, J. L. (2018). Interaction of Waves with Idealized High-Relief
- Bottom Roughness. Journal of Geophysical Research: Oceans, 123(4), 3038-3059.

1573

- Zawada, D. G., & Brock, J. C. (2009). A multiscale analysis of coral reef topographic
- 1575 complexity using lidar-derived bathymetry. Journal of Coastal Research, 6-15.

1576

## 1578 Figures

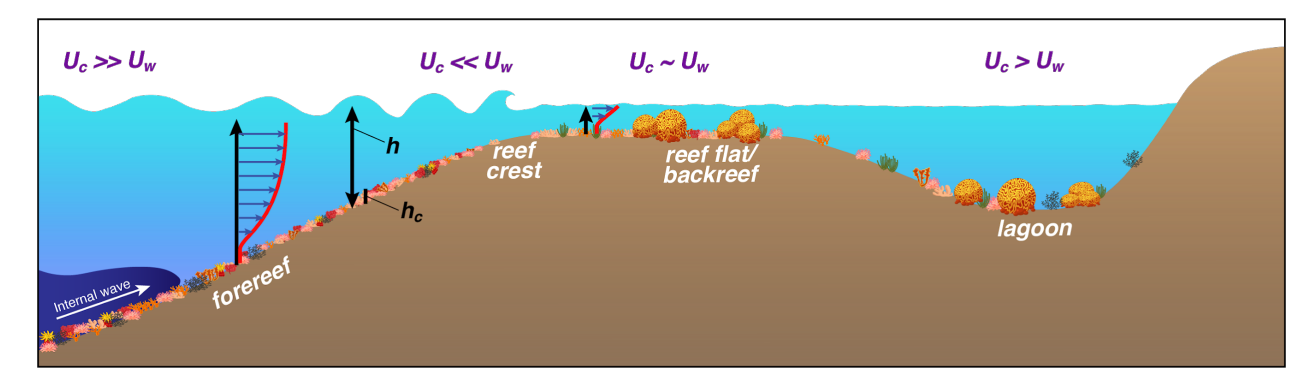
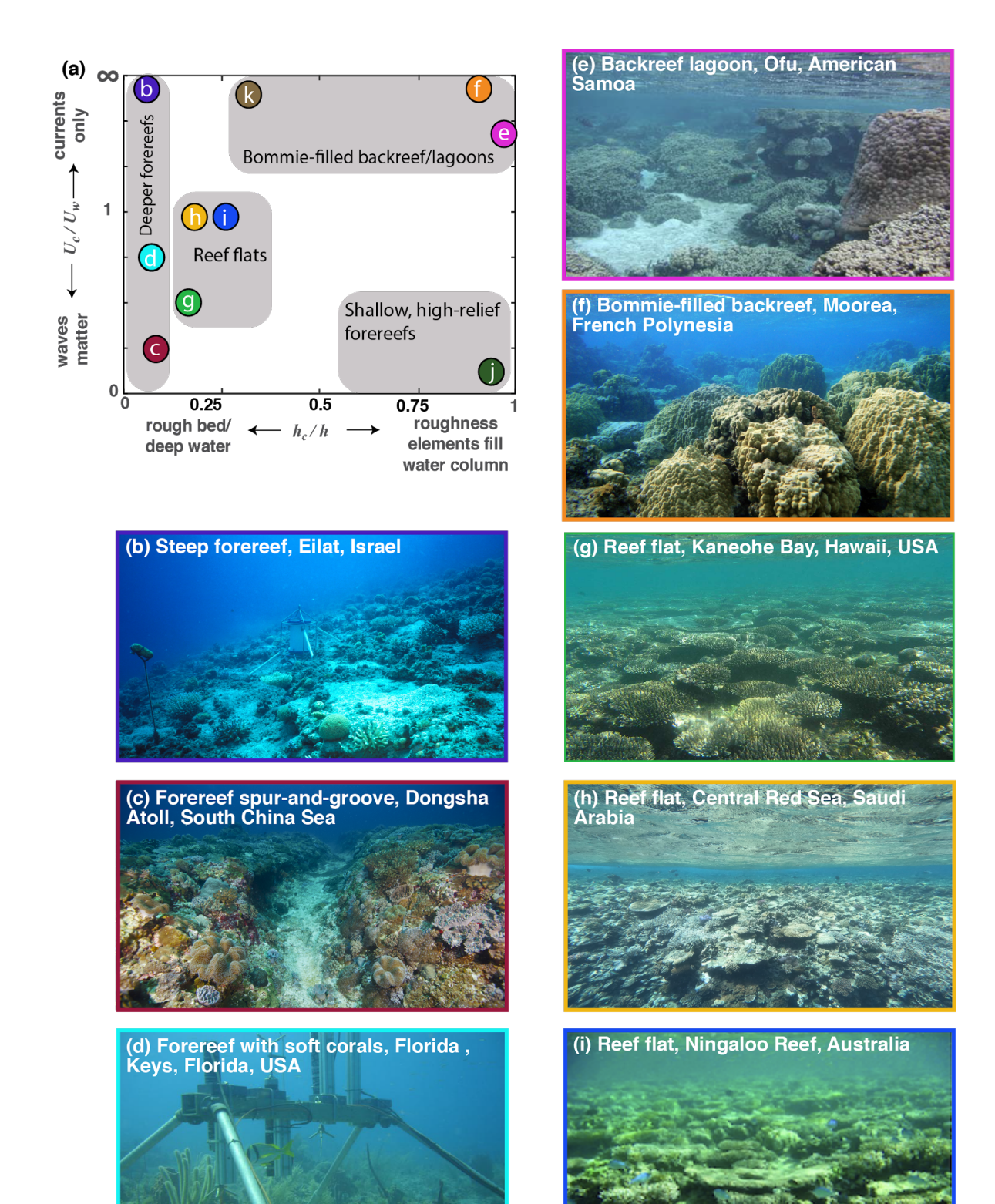


Figure 1. – Schematic of a coral reef system with some common biogeographic zones: the deep forereef where mean flows are often oriented alongshore, the shallow forereef/reef crest which is heavily influenced by the energetic dissipation of wave energy, the reef flat/back reef zone where flow is driven by wave setup offshore and tidal flows and coral canopies can fill the entire water column, and deeper lagoons where flow is fairly tranquil and sheltered from waves. Each zone of the reef is characterized by relative magnitudes of steady ( $U_c$ ) to oscillatory ( $U_w$ ) flow velocities.



1591 Figure 2. – (a) Coral reef environments classified by flow environment and roughness ratio 1592 for studied reef locations pictured in (b) Eilat, Israel (Reidenbach et al. 2006), (c) Dongsha 1593 Atoll, Taiwan, South China Sea (Reid et al. 2019; Davis et al. 2020) (d) Conch Reef, 1594 Florida, USA (Davis & Monismith 2011) (e) Ofu, American Samoa (Rogers et al. 2018; 1595 Green 2002), (f) Moorea, French Polynesia (Hench & Rosman 2013), (g) Kaneohe Bay, 1596 Hawaii, USA (Lowe et al. 2005a), (h) Central Red Sea, Saudi Arabia (Lentz et al. 2016, 1597 2017), (i) Ningaloo Reef, Australia (Taebi et al. 2011; Pomeroy et al. 2012), and not 1598 pictured, but plotted in (a): point (j) Ipam, Guam (Pequignet et al. 2011) and point (k) 1599 Lady Elliot Island, Australia (Huang et al. 2012). 1600



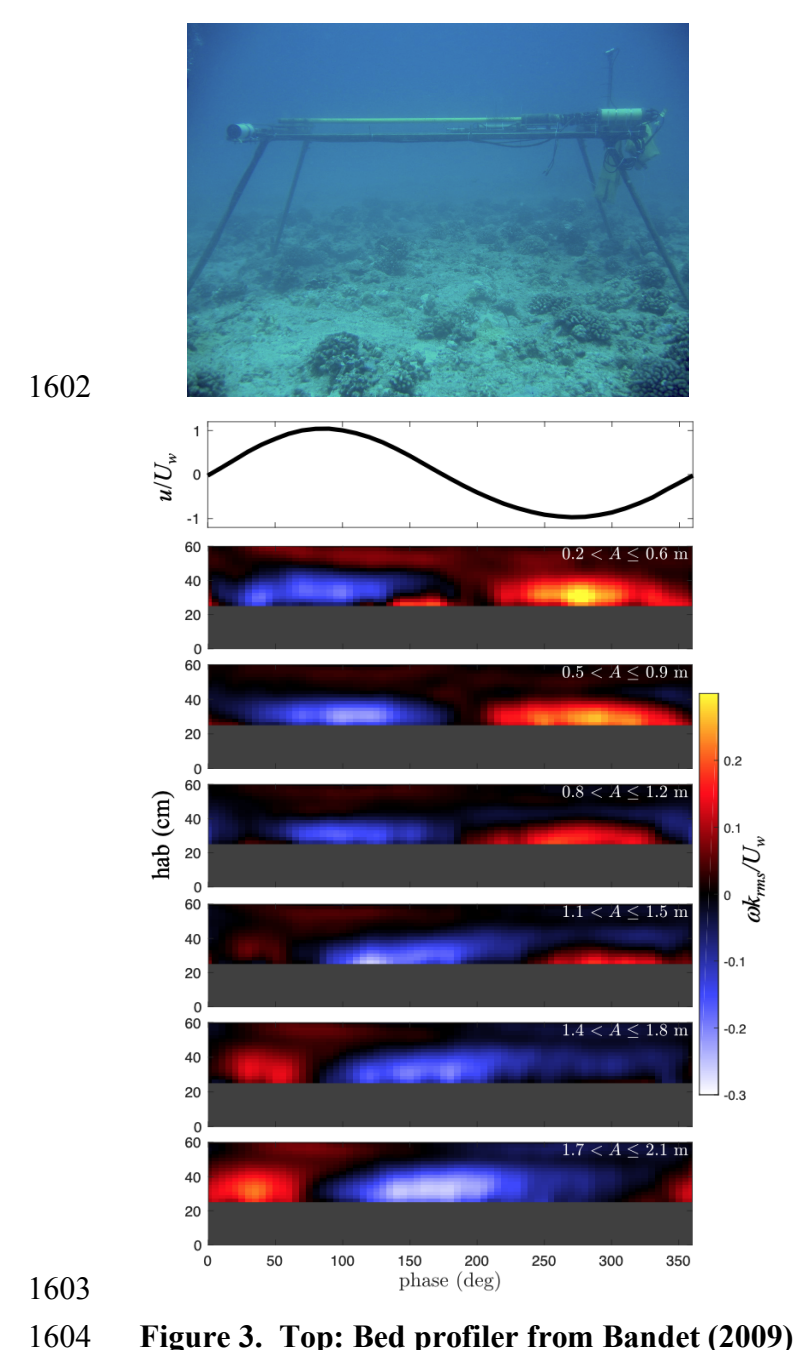


Figure 3. Top: Bed profiler from Bandet (2009). Bottom: Phase averaged wave boundary layer structure over a rough coral reef surface pictured at top. Upper panel shows cross-shore normalized wave velocity (60 cm above the bottom). Six lower panels show near-bed normalized spatially averaged vorticity versus average height above bed over a 2m transect for increasing wave orbital amplitude, A.

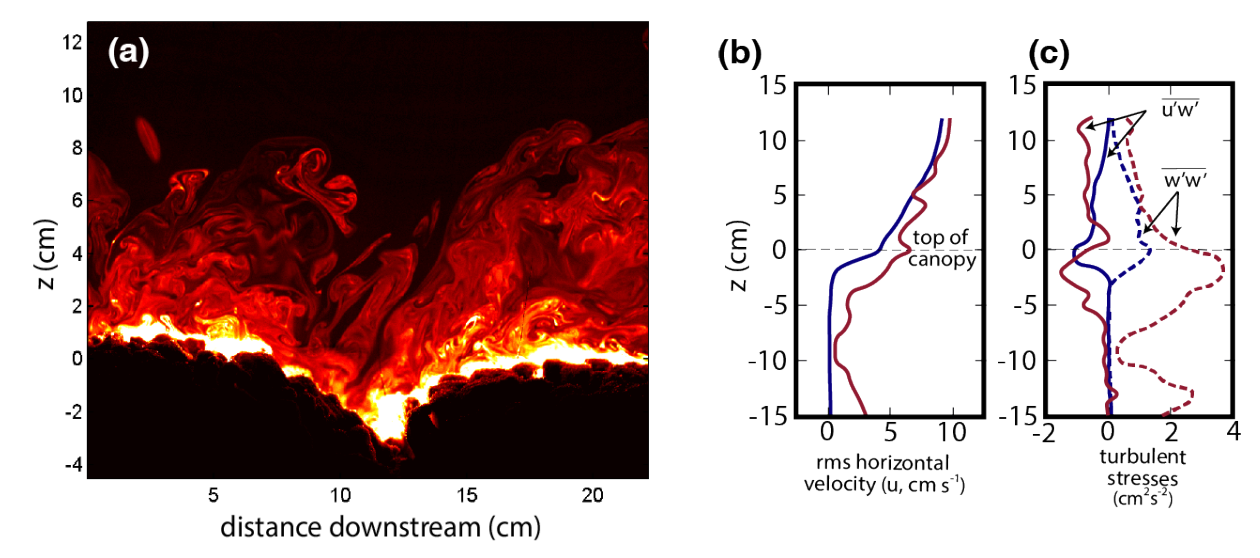


Figure 4. (a) Turbulent structures visualized with planar laser induced fluorescence (PLIF) in a region at the interface between a canopy of *Porites compressa* coral skeletons in an oscillatory flow. (b) root-mean-square (rms) horizontal velocity for a unidirectional flow run with mean downstream flow of  $U_c = 8.5$  cm s<sup>-1</sup>(blue lines) and a wave-dominated flow with wave period, T = 5 s, and wave orbital velocity amplitudes,  $U_w = \pm 9$  cm s<sup>-1</sup>(red lines), (c) turbulent stresses  $(\overline{u'w'})$  and  $\overline{w'w'}$  measured within and above coral canopy. Image and data from Reidenbach et al. (2007, used with permission).

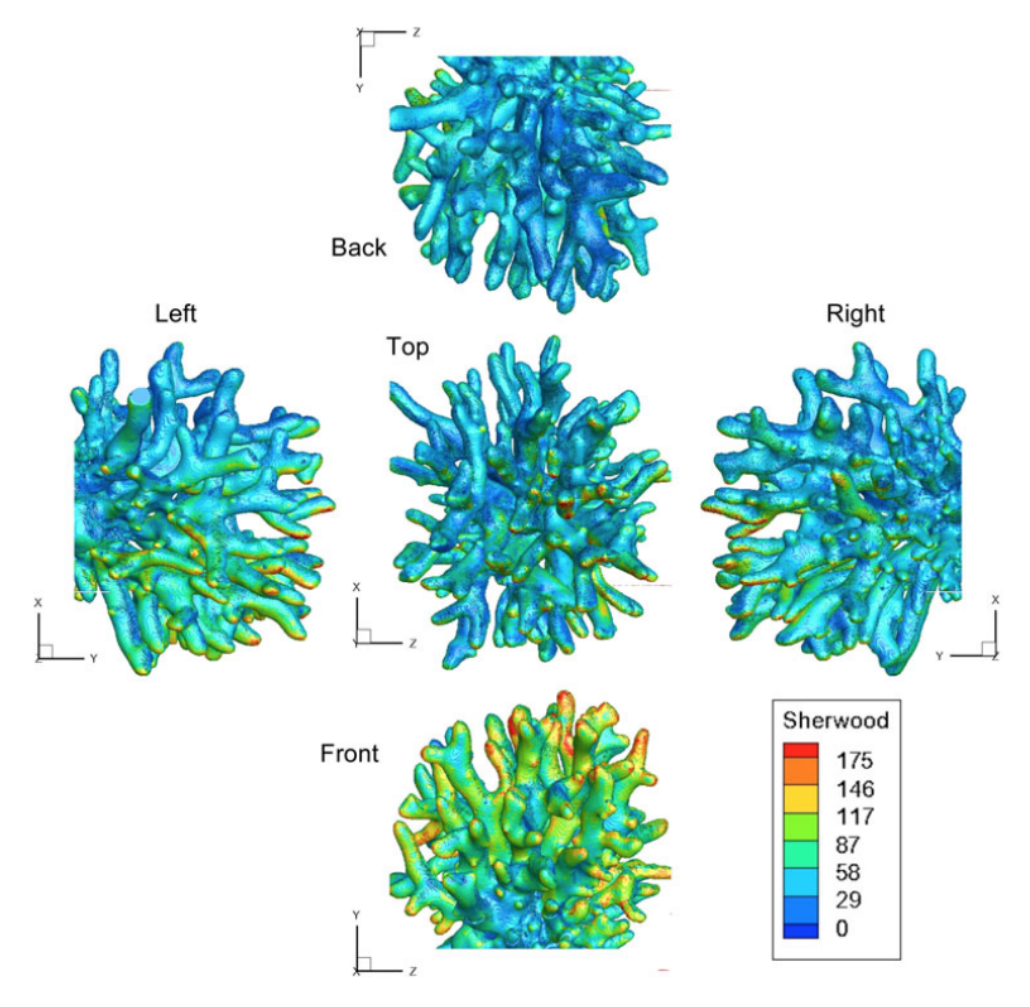


Figure 5. Local mass transfer (normalized by diffusive transfer rate, as the dimensionless Sherwood number) for a *Stylophora pistillata* colony immersed in a steady flow in a flume (from Chang et al. 2013, used w. permission).

1626 Table 1. Summary of variables used in this review

		iables used in this review
Variable	Unit	Description
A	m	Wave orbital amplitude
$A_T$	m <sup>2</sup>	Total plan area of bed
b	m	Characteristic lateral roughness spacing
C	kg m <sup>-3</sup>	Concentration of a scalar
$C_D$	-	Coefficient of drag
$C_d$	-	Coefficient of drag associated with canopy structure
D	N	Drag force
$f_e$	-	Wave energy dissipation factor
f <sub>e</sub> f <sub>w</sub>	-	Wave friction factor
F	kg m <sup>-2</sup> s <sup>-1</sup>	Flux of a scalar
$F_x$	m s <sup>-2</sup>	Spatially averaged drag force per volume exerted by the canopy on the flow
h	m	Water depth
$h_c$	m	Canopy height
$K_t$	$m^2 s^{-1}$	Turbulent diffusivity of a scalar
k	m	Characteristic physical roughness length scale
$k_s$	m	Characteristic/equivalent sand grain roughness
$L_c$	m	Characteristic horizontal scale for heterogeneity
p	N m <sup>-2</sup>	Pressure
P	-	Roughness parameter
S	m	Characteristic lateral roughness length scale
T	S	Wave period
t	S	Time
$\boldsymbol{u} = [u, v, w]$	m s <sup>-1</sup>	Flow velocity in 3D space, $x = [x, y, z]$
$u_*$	m s <sup>-1</sup>	Friction or shear velocity
U	m s <sup>-1</sup>	Characteristic flow velocity
$U_{\delta b}$	m s <sup>-1</sup>	Velocity at the blending height
$U_c$	m s <sup>-1</sup>	Characteristic steady, unidirectional flow velocity
$U_w$	m s <sup>-1</sup>	Characteristic oscillatory flow velocity
$V_t$	m s <sup>-1</sup>	Mass transfer velocity
W	m	Characteristic roughness spacing
$z_0$	m	Hydrodynamic roughness
$Z_{ref}$	m	Hydrodynamic origin or displacement height
δ	m	Boundary layer thickness
$\delta_b$	m	Blending height
$\mathcal{E}_f$	$m^2$ s <sup>-3</sup>	Dissipation of wave energy due to bed friction
à	-	Roughness density, frontal area of elements per plan area.
μ	kg m <sup>-1</sup> s <sup>-1</sup>	Fluid viscosity
V	$m^2$ s <sup>-1</sup>	Kinematic viscosity
$v_t$	$m^2$ s <sup>-1</sup>	Turbulent diffusivity of momentum
$\phi_{wc}$	radians	Angle between waves and steady current
	kg m <sup>-3</sup>	Fluid density
ρ	rg III	1 full defisity

$ au_{XZ}$	kg m <sup>-1</sup> s <sup>-2</sup>	Shear stress
$ au_b$	kg m <sup>-1</sup> s <sup>-2</sup>	Shear stress at the bed
ω	s <sup>-1</sup>	Vorticity
ζο	m	Hydrodynamic origin (relative to top of roughness)